Accepted Manuscript

Global distribution of the HIMU end member: Formation through Archean plume-lid tectonics

Stephan Homrighausen, Kaj Hoernle, Folkmar Hauff, Jörg Geldmacher, Jo-Anne Wartho, Paul van den Bogaard, Dieter Garbe-Schönberg

PII:	S0012-8252(17)30294-5
DOI:	doi:10.1016/j.earscirev.2018.04.009
Reference:	EARTH 2619
To appear in:	*Earth-Science Reviews*
Received date:	2 June 2017
Revised date:	31 March 2018
Accepted date:	25 April 2018

Please cite this article as: Stephan Homrighausen, Kaj Hoernle, Folkmar Hauff, Jörg Geldmacher, Jo-Anne Wartho, Paul van den Bogaard, Dieter Garbe-Schönberg , Global distribution of the HIMU end member: Formation through Archean plume-lid tectonics. The address for the corresponding author was captured as affiliation for all authors. Please check if appropriate. Earth(2018), doi:10.1016/j.earscirev.2018.04.009

Global distribution of the HIMU end member: Formation through Archean Plume-lid Tectonics

Stephan Homrighausen[1*], Kaj Hoernle[1,2], Folkmar Hauff[1], Jörg Geldmacher[1], Jo-Anne Wartho[1], Paul van den Bogaard[1], Dieter Garbe-Schönberg[2]

[1]GEOMAR Helmholtz Centre for Ocean Research Kiel, Wischhofstr. 1-3, 24118 Kiel, Germany

[2]Christian-Albrechts-University of Kiel, Ludewig-Meyn-Str. 10, 24118 Kiel, Germany

*Corresponding author (shomrighausen@geomar.de)

Abstract

Oceanic basalts reflect the heterogeneities in the earth's mantle, which can be explained by five mantle end members. The HIMU end member, characterized by high time-integrated μ ($^{238}U/^{204}Pb$), is defined by the composition of lavas from the ocean islands of St. Helena, South Atlantic Ocean and Mangaia and Tubuai (Cook-Austral Islands), South Pacific Ocean. It is widely considered to be derived from a mantle reservoir that is rarely sampled and not generally involved in mixing with the other mantle components. On the other hand, the FOZO end member, located at the FOcal ZOne of oceanic volcanic rock arrays on isotope diagrams, is considered to be a widespread common component with slightly less radiogenic $^{206}Pb/^{204}Pb$ and intermediate Sr-Nd-Hf isotopic compositions. Here we present new major and trace element, Sr-Nd-Pb-Hf isotope and geochronological data from the Walvis Ridge and Richardson Seamount in the South Atlantic Ocean and the Manihiki Plateau and Eastern Chatham Rise in the southwest Pacific Ocean. Our new data, combined with literature data, document a more widespread (nearly global) distribution of the HIMU end member than previously postulated. Our survey shows that HIMU is generally associated with low-volume alkaline, carbonatitic and/or kimberlitic intraplate volcanism, consistent with derivation from low degrees of melting of CO_2-rich sources. The majority of end member HIMU locations can be directly related to hotspot settings. The restricted trace element and isotopic composition (St. Helena type HIMU), but near-global distribution, point to a deep-seated, widespread reservoir, which most likely formed in the Archean. In this context we re-evaluate the origin of a widespread HIMU reservoir in an Archean geodynamic setting. We point out that the classic ocean crust recycling model cannot be applied in a plume-lid dominated tectonic setting, and instead

propose that delamination of carbonatite- metasomatized subcontinental lithospheric mantle could be a suitable HIMU source.

Keywords: HIMU; FOZO; Walvis Ridge; Chatham Rise; Manihiki Plateau; Shona hotspot

1. Introduction

Incompatible elements and Sr-Nd-Pb-Hf isotope compositions of mafic oceanic basalts have been used to identify at least four mantle end members that can explain the large-scale geochemical heterogeneity of the Earth's mantle. These are 1) Depleted Mantle (DM), 2) mantle with high time-integrated μ ($^{238}U/^{204}Pb$; HIMU), 3) Enriched Mantle One (EMI), and 4) Enriched Mantle Two (EM II) (Zindler and Hart, 1986; Hofmann, 1997; White, 2015). Since Mid-Ocean Ridge Basalts (MORBs) and many ocean island basalts (OIBs) converge on an intermediate Sr-Nd-Pb isotopic composition, the concept of a "common" (C, Hanan and Graham, 1996) or "prevalent" (PREMA, Zindler and Hart, 1986; Stracke, 2012) mantle component has been proposed. This "omnipresent" mantle component, which we refer to as FOZO (FOcal ZOne; Hart et al., 1992) henceforth after Stracke et al. (2005), lies within the isotopic space of DM, HIMU, EM. In some cases FOZO has been associated with high $^{3}He/^{4}He$ (> 9 R/Ra), leading some to propose that it may be a distinct mantle end member rather than a mix of the other end members (e.g. Zindler and Hart, 1986; Hart et al., 1992; Hanan and Graham, 1996).

The HIMU mantle end member is defined by the composition of lavas from the ocean islands of St. Helena in the South Atlantic Ocean, and of Mangaia and Tubuaii (hereafter termed Cook-Austral) in the Southwest Pacific Ocean (Zindler and Hart, 1986; Chaffey et al., 1989; Woodhead, 1996). This end member is characterized by radiogenic $^{206}Pb/^{204}Pb$ (> 20.5) and $^{207}Pb/^{204}Pb$ (> 15.7), but $^{208}Pb/^{204}Pb$ ratios well below the Northern hemisphere reference line (Hart, 1984) and Sr-Nd-Hf isotope ratios projecting beneath the EM-DM mantle array (e.g., Zindler and Hart, 1986; Woodhead, 1996; Stracke et al., 2005; Kawabata et al., 2011; Hanyu et al., 2014; White, 2015). Its isotopic composition must reflect long-term, time-integrated enrichment of U and Th relative to

Pb (~1.0–3.2 Ga; e.g., Tatsumoto, 1978; Hofmann, 1997; Stracke et al., 2005; Hanyu et al., 2011; Cabral et al., 2013; Nebel et al., 2013; Castillo, 2015), coupled with time-integrated low Th/U and Rb/Sr ratios, but moderate Sm/Nd and Lu/Hf ratios. It should be noted that we use the term end member HIMU in this manuscript to refer to the composition of the reference HIMU localities of St. Helena and Cook-Austral Islands as is common in the literature, while recognizing that the "real end member" could have more extreme compositions than the reference localities.

It is widely accepted that HIMU represents a rare mantle end member, whereas the prevalent FOZO end member is a common mixing component present in MORBs and OIBs (e.g., Hart et al., 1992; Hanan and Graham, 1996; Stracke et al., 2005; Stracke, 2012). In the last few decades numerous models were proposed to explain the restricted and unique composition of HIMU (e.g., Zindler and Hart, 1986; Chauvel et al., 1992; Stracke et al., 2003; Pilet et al., 2005; Willbold and Stracke, 2006; Hanyu et al., 2011; Castillo, 2015), whereas FOZO (also termed "Young HIMU"; Thirlwall, 1997) is usually explained by a similar reservoir formation mechanism, but with overall younger formation ages compared to HIMU (e.g., Thirlwall, 1997; Stracke et al., 2005; Castillo, 2015).

In the classic ocean crust-recycling model, the combination of hydrothermal alteration and subduction modification/slab dehydration are proposed to produce these unique trace element ratios in the subducting oceanic slab, followed by long-term storage in the lower mantle and eventual ascent to the surface in mantle plumes (e.g., Hofmann and White, 1982; Zindler and Hart, 1986; Chauvel et al., 1992; Stracke et al., 2003; Cabral et al., 2013; Hanyu et al., 2014; Kimura et al., 2016). Several observations, however, challenge this model. First, recycled oceanic crust transforms under mantle conditions to eclogite/pyroxenite, but these source lithologies alone cannot generate

partial melts with the characteristic HIMU major element composition (e.g., Jackson and Dasgupta, 2008; Dasgupta et al., 2010; Mallik and Dasgupta, 2012). Instead, low Ni concentrations and high Mn/Fe and Ca/Al ratios in olivine phenocrysts from HIMU lavas indicate that peridotite is the dominate source lithology (Herzberg et al., 2014; Weiss et al., 2016). Another problem with the ocean-crust-recycling model is that MORB does not trend towards the HIMU reference localities on Pb isotope diagrams (e.g. $^{206}Pb/^{204}Pb$ versus $^{208}Pb/^{204}Pb$ and $^{87}Sr/^{86}Sr$), precluding a simple relation between HIMU and MORB (Stracke et al., 2005; Castillo, 2015; Weiss et al., 2016). In addition, Hanyu et al. (2011) stated that recycled oceanic crust has extremely high Re/Os ratios and after billions of years the $^{187}Os/^{188}Os$ should be highly evolved (> 1) relative to chondrites and the average earth's mantle (~0.127). In their model, mixing of pure recycled and long-term isolated oceanic crust with the depleted mantle cannot reproduce the observed Os-Pb-Hf systematics of HIMU lavas ($^{187}Os/^{188}Os$ ratios of 0.14-0.15).

In response to these critical observations, several alternative explanations for the origin of the HIMU source were introduced (e.g., Pilet et al., 2005; Collerson et al., 2010; Hanyu et al., 2011; Castillo, 2015; Weiss et al., 2016). For example, Pilet et al. (2005) proposed that metasomatized recycled oceanic lithosphere could represent the HIMU source. Castillo (2015) argued that small amounts of recycled Archean marine carbonates are the main source of HIMU. Alternatively, it has been proposed that HIMU could develop within the (peridotitic) subcontinental lithospheric mantle (SCLM) by infiltration of (carbonatitic) fluids and/or melts (e.g., Hart et al., 1986; Stein et al., 1997; Lucassen et al., 2008; Rooney et al., 2014; McCoy-West et al., 2016; Weiss et al., 2016). However, all these various HIMU reservoir formation models have one thing in common - that the formation of HIMU is associated to modern-style tectonics. Recently, Cabral et al. (2013) showed that the negative $\Delta^{33}S$ ratios in olivines from Cook-Austral HIMU lavas

require their source to be ≥2.45 Ga with ages of up to 3.2 Ga being proposed by Nebel et al. (2013). The style of Archean plate tectonics, however, remains highly controversial (Foley et al., 2003; Bédard, 2006; Van Kranendonk, 2010; Gerya, 2014; Harris and Bédard, 2014; Moyen and Laurent, 2018) and it is questionable if modern-style plate tectonics can be used as an analog.

In this study we report new geochemical and geochronological data from selected submarine lavas, recovered during five cruises with German research vessels (R/V Maria S. Merian and R/V Sonne), and show that these samples have a St. Helena HIMU end member composition. Combined with literature data, we demonstrate that end member HIMU is an almost globally distributed mantle end member reflecting a widespread reservoir(s) in the lowermost mantle. Based on proposed reservoir formation ages of >2.45 Ga (Cabral et al., 2013; Nebel et al., 2013; Castillo, 2015), we re-evaluate the formation of a globally distributed HIMU end member in the context of the Archean geodynamic setting.

2. Geological background of the sample locations

We recovered submarine lavas from five cruises with German research vessels: Cruises SO84 and SO233 to the Walvis Ridge, South Atlantic, cruise MSM19/3 with the R/V Maria S. Merian to Richardson seamount, South Atlantic, cruise SO193 to the Manihiki plateau, SW Pacific, and cruise SO168 with the R/V Sonne to the Eastern Chatham Rise, SW Pacific. In the following we present a brief geological background of the respective sample locations.

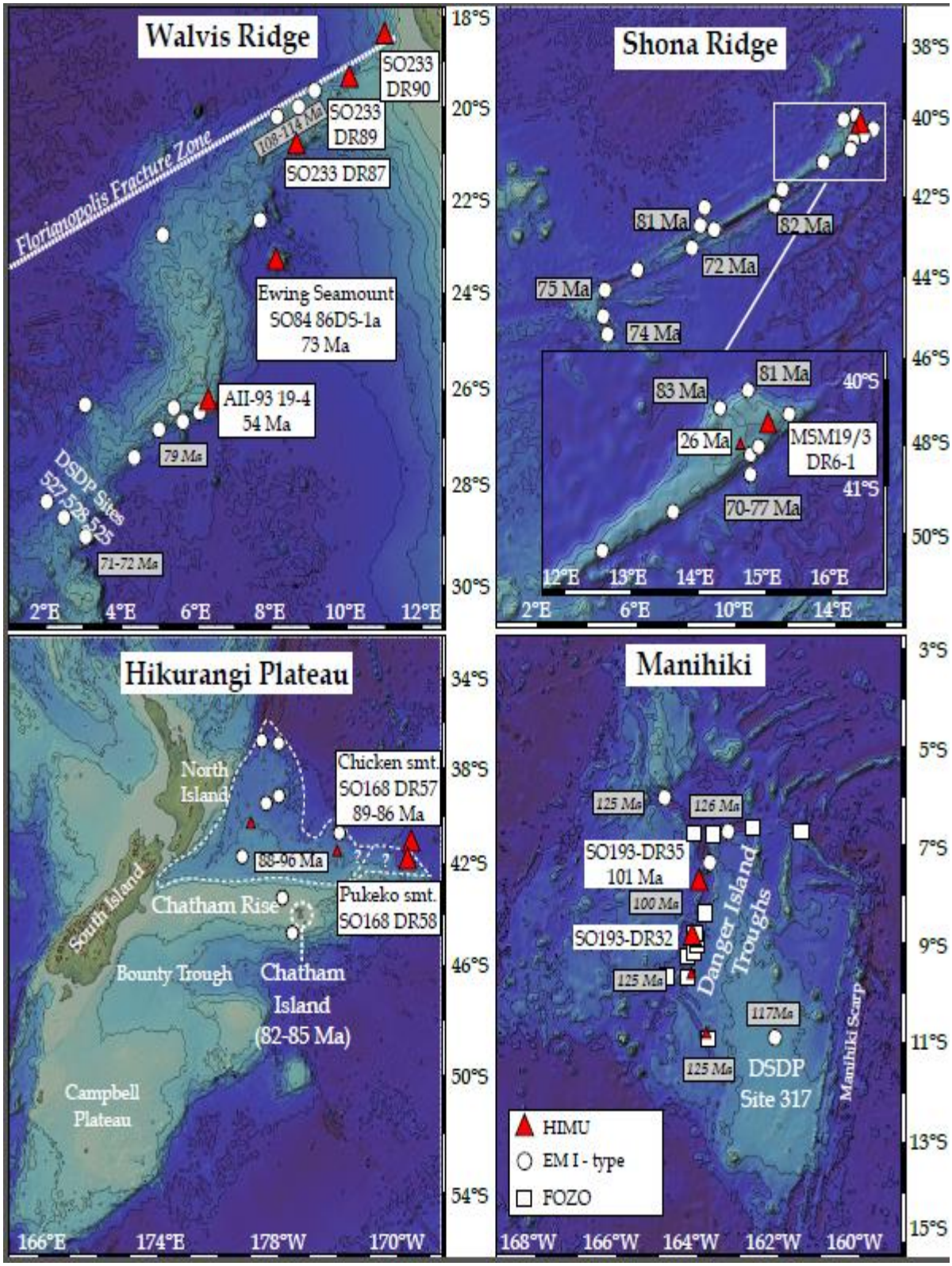

Fig. 1: Maps of the Walvis Ridge, Manihiki Plateau, Hikurangi Plateau and Shona Ridge/Richardson seamount with sample sites from the respective cruises (red triangles). Sample sites from the literature with 1) EM I-type compositions are shown as white circles, 2) HIMU with small red triangles and 3) FOZO compositions with squares. Source of bathymetric map:

http://www.geomapapp-org. Sample sites and age data: Walvis Ridge (Richardson et al., 1984; Thompson and Humphris, 1984; Salters and Sachi-Kocher, 2010; Rohde et al., 2013a; Rohde et al., 2013b; Hoernle et al., 2015; O'Connor and Jokat, 2015a, b), Manihiki plateau (Ingle et al., 2007; Hoernle et al., 2010; Timm et al., 2011; Golowin et al., 2017), Zealandia and Hikurangi Plateau (Panter et al., 2006; Hoernle et al., 2010; Timm et al., 2010) and Shona Ridge/Richardson seamount (Le Roex et al., 2010; O'Connor et al., 2012; Hoernle et al., 2016).

[Two columns]

2.1 The Walvis Ridge

The continuous aseismic Walvis Ridge represents the oldest submarine expression of the age progressive Tristan-Gough hotspot track (Rohde et al., 2013a; Rohde et al., 2013b; Hoernle et al., 2015; O'Connor and Jokat, 2015a), which extends from the Parana and Etendeka flood basalt provinces to the Walvis Ridge and then to the Guyot Province, ending at the active volcanic islands of Tristan da Cuhna and Gough. The age progression is the strongest evidence that the track was formed by a mantle plume, which is supported by recent seismic tomographic data that images a low-velocity conduit-like structure with a radius of 100 km down to a depth of 250km, just to the southwest of Tristan da Cunha (Schlömer et al., 2017). This shallow velocity anomaly lies above a broader vertically continuous conduit-like structure with ∂V_S ratios of < -0.5% in the depth range of 1000-2800 km (French and Romanowicz, 2015). High $^3He/^4He$ ratios (> 10 R_A) from olivines in Etendeka flood basalts provide further support for a lower mantle origin (Stroncik et al., 2017).

Consistent with the mantle plume model (e.g., Wilson, 1963; Morgan, 1971; Richards et al., 1989), the Tristan-Gough hotspot track initiated with the Etendeka and Parana flood basalt provinces at ~135 Ma (Renne et al., 1996) and were subsequently split apart by seafloor spreading related to the opening of the South Atlantic Ocean. Thereafter, the mantle plume interacted with the Mid-Atlantic ridge, forming the Walvis Ridge and Rio Grande Rise (120-60 Ma, Humphris and Thompson, 1983; O'Connor and Duncan, 1990; Rohde et al., 2013a; Hoernle et al., 2015; O'Connor and Jokat, 2015a, b) and since ~60 Ma became intraplate forming the Guyot Province, which connects the Walvis Ridge with the active volcanic islands of Tristan da Cunha and Gough.

The last 70 Ma of the Tristan-Gough hotspot track shows geochemical zonation primarily in Pb isotopic composition (Rohde et al., 2013a; Hoernle et al., 2015) with the zonation beginning at the DSDP Site transect at the SW end of the Walvis Ridge (Fig. 1). Both compositional types (Tristan and Gough) lie within the compositional range of EM I. In the >70 Ma portion of the Walvis Ridge hotspot track (there are few available samples from the Rio Grande Rise), only Gough-type compositions have been documented thus far (e.g., Hoernle et al., 2015). DSDP Site 525 (Gough-type) on the southern Walvis Ridge is considered to be the Atlantic type locality for the EM I end member (e.g., Zindler and Hart, 1986; White, 2015).

The top of the central portion of the Walvis Ridge, Valdivia Bank, and the northeastern end of the Walvis Ridge are flat (Hoernle et al., 2014), suggesting that these parts of the Walvis Ridge were once subaerially exposed and eroded to sea level. Seamounts on the Walvis Ridge postdate this erosional stage and thus must be significantly younger in age than the Walvis Ridge basement. $^{40}Ar/^{39}Ar$ dating shows that late-stage (post-erosional) volcanism on (sample AII-93-19-4; Rohde et al., 2013b) and adjacent to the Walvis Ridge (sample SO84 86DS-1a; O'Connor and Jokat, 2015a) is ~30 Ma younger than the corresponding ridge basement (geochemical data for both samples in Appendix B). During R/V Sonne cruise SO233, three late-stage seamounts were sampled by dredging (Fig.1): Two seamounts (SO233 dredge locations DR87 and DR89) are located on the flat northeastern part of the Walvis Ridge. A third seamount (SO233 dredge station DR90) is located on the seafloor northwest of the Florianopolis Fracture Zone (FFZ). As a result of several ridge jumps, the oceanic crust northwest of this fracture zone became part of the South American plate. The ocean crust beneath the seamount dredged at SO233 DR90 is estimated to be ~93 Ma (O'Connor and Jokat, 2015b), providing a maximum age for this seamount and sample (Fig.1).

2.2 Richardson Seamount (Shona hotspot track)

Richardson seamount (69-84 Ma) is located ~2000 km south of the Walvis Ridge and belongs to the Shona hotspot track (Fig. 1; O'Connor et al., 2012; Hoernle et al., 2016). Samples from the older part of the Shona hotspot track have an EM I-type geochemical signature, similar to the Gough subtrack and most of the Walvis Ridge basement (Hoernle et al., 2016). Several small late-stage cones are located on the flat (erosional) top of this elongated guyot, post-dating erosion to sea level and subsequent subsidence. An $^{40}Ar/^{39}Ar$ age of 26 ± 0.3 Ma (2σ) was obtained from one of these post-erosional cones (O'Connor et al., 2012), which is ≥ 40 Ma younger than the guyot basement (Hoernle et al., 2016). We assume a similar age for our sample MSM19/3 DR6-1 from a nearby post-erosional cone, since it has the same tectonic setting and similar major and trace element characteristics to the dated sample (D35-1; Le Roex et al., 2010).

2.3 The Manihiki-Hikurangi plateau seamounts

Seafloor fabric data, similar formation ages (~123-116 Ma), plate tectonic reconstructions and geochemical data suggest that the Ontong-Java, Hikurangi and Manihiki oceanic plateaus were once part of a giant plateau, which may have been emplaced by a massive mantle upwelling (Fig. 1; e.g. Taylor, 2006; Davy et al., 2008; Hoernle et al., 2010; Timm et al., 2011; Chandler et al., 2015; Hochmuth et al., 2015; Golowin et al., 2017). The basements of these three oceanic plateaus are characterized by EM I-type affinities, with various sub-groups (e.g., Kwaimbaita-, Kroenke-, Singallo-type; see Tejada et al., 1996; Tejada et al., 2002; Hoernle et al., 2010; Timm et al., 2011; Jackson et al., 2015; Golowin et al., 2017 for a detailed description). The Manihiki

basement rocks show evidence of a HIMU-type component (Timm et al., 2011; Golowin et al., 2017). After the combined Ontong Java – Manihiki – Hikurangi Plateau broke into the three respective plateaus (Taylor, 2006; Davy et al., 2008; Chandler et al., 2015; Hochmuth et al., 2015), the Hikurangi plateau drifted southward until it collided with the Eastern Gondwana margin and clogged this subduction system at ~105 Ma (Bradshaw, 1989; Davy et al., 2008; Hoernle et al., 2010).

In contrast to the tholeiitic basement lavas, alkalic volcanism is present in the form of seamounts on Manihiki and Hikurangi Plateaus and dikes in the Ontong Java Plateau, largely emplaced between 110-65 Ma (Beiersdorf et al., 1995; Tejada et al., 1996; Tejada et al., 2002; Ingle et al., 2007; Hoernle et al., 2010; Pietsch and Uenzelmann-Neben, 2015). On the Hikurangi plateau, the seamounts formed primarily between 99-87 Ma (Hoernle et al., 2010) followed by rifting and seafloor spreading that separated the blocked portion of the Gondwana subduction zone (Zealandia) from West Antarctica beginning at ≥ 85 Ma (Davy et al., 2008; Hoernle et al., 2010). Gondwana breakup was accompanied by volcanism on the Chatham Islands taking place between 85-82 Ma (Panter et al., 2006). Several models argue that breakup between Zealandia and Antarctica was triggered by a mantle plume with a HIMU signature beneath the Gondwana margin during the Late Cretaceous (Weaver et al., 1994; Hart et al., 1997; Storey et al., 1999; Panter et al., 2006; Hoernle et al., 2010; Kipf et al., 2014).

During the R/V Sonne SO193 cruise, samples from late-stage volcanic centers on the western flank of the prominent Danger Island Troughs graben system of the Manihiki plateau were recovered (Werner and Hauff, 2007). Since both seamounts are located at the edge of the en echelon Danger Island Troughs, we assume a causal relationship to the rift zone dissecting the Manihiki plateau between 118 – 100 Ma

(Taylor, 2006; Ingle et al., 2007; Timm et al., 2011; Hochmuth et al., 2015), suggesting that the seamounts formed within this time interval.

During R/V Sonne SO168 cruise, one seamount was sampled by dredging on the easternmost portion of the Chatham Rise (Pukeko Seamount; SO168 DR58) and one just north of the Eastern Chatham Rise (Chicken/Hühnchen Seamount; SO168 DR57; Hoernle et al., 2003; Fig.1). Both seamounts are assumed to sit on the stretched and thinned continental crust of the Eastern Chatham Rise (part of Zealandia), which was affected by the sudden change from the collision with the Hikurangi plateau and following break up from Antartica (e.g. Bradshaw, 1989; Weaver et al., 1994; Davy et al., 2008). The Chicken Seamount is a guyot with a flat top (2000 m below sea level) most likely formed by wave base abrasion, whereas the smaller Pukeko Seamount has a ridge-type structure and is 300 m lower than Chicken and possibly never reached sea level (Hoernle et al., 2003).

3. Analytical methods

Details about sample preparation; $^{40}Ar/^{39}Ar$ age dating and geochemical (major and trace element and radiogenic isotope) methods are reported in Appendices A-E. In the following section, we present the $^{40}Ar/^{39}Ar$ age data derived from the submarine samples from the Eastern Chatham Rise and Manihiki plateau seamount(s). Afterwards, we evaluate the potential effects of seawater alteration and describe the method we used to compare HIMU localities over an age range of ~130 Ma.

3.1. $^{40}Ar/^{39}Ar$ dating

We report the results of two new $^{40}Ar/^{39}Ar$ ages from Eastern Chatham Rise and Manihiki plateau using acid-leached plagioclase separates. We monitored the Ca/K ratios and calculated $^{36}Ar/^{37}Ar$ plagioclase alteration index (AI) values (Baksi, 2007; van

den Bogaard, 2013). We used the calculated $^{36}Ar/^{37}Ar$ plagioclase Alteration Index (AI) cut-off value of 0.00006 (Baksi, 2007; van den Bogaard, 2013), and the percent of atmospheric ^{40}Ar ($^{40}Ar_{atm}$) values to determine the degree of alteration of the laser step-heating or total fusion analyses. Inverse isochron ages were calculated to confirm both the plateau and total fusion ages and identify if the samples preserved initial atmospheric $^{40}Ar/^{36}Ar$ ratios, without the presence of extraneous ^{40}Ar components (i.e., an atmospheric $^{40}Ar/^{36}Ar$ ratio of 295.5; Steiger and Jäger, 1977).

We consider $^{40}Ar/^{39}Ar$ step-heating analyses as statistically valid if the following widely accepted criteria are fulfilled (e.g., Lanphere and Dalrymple, 1978; Pringle et al., 1993; O'Connor and Jokat, 2015b): (1) a well-defined age spectrum plateau created by three or more continuous and concordant steps (at the 2σ confidence level) with > 50% of the cumulative ^{39}Ar, (2) the mean square of weighted deviations (MSWD) is ≤ 2, and the probability (P) of fit is > 0.05, and (3) the calculated plateau and isochron ages are concordant at 95 % confidence levels (Table 1; Appendix C).

Plagioclase step-heating of sample SO193 DR35-1 (Manihiki plateau) yields a statistically valid plateau age of 100.70 ± 0.93 Ma (2σ; MSWD = 1.60; P = 0.18; 61.9 % ^{39}Ar). All plateau steps yield high $^{36}Ar/^{37}Ar$ AI values, above the plagioclase $^{36}Ar/^{37}Ar$ cut-off value of 0.00006 (Baksi, 2007), and elevated ^{40}Ar atmospheric ($^{40}Ar_{atm}$) values, indicating the degassing of Ar from altered material. The statistically invalid inverse isochron age of 100.3 ± 3.3 Ma (95% conf.; MSWD = 7.9; P = 0.00; initial $^{40}Ar/^{36}Ar$ = 298 ± 16; Spreading Factor (SF) = 43.0%), however, confirms the plateau age. Due to the alteration of this sample, the $^{40}Ar/^{39}Ar$ plateau age of sample SO193 DR35-1 of 100.70 ± 0.93 Ma (2σ) should be treated with some caution, but this plateau age lies within the age range of the formation of the Danger Island Troughs (118-100 Ma).

Laser total fusion $^{40}Ar/^{39}Ar$ dating of 5 plagioclase analyses (weighing between 0.18-0.42 mg) from the Chicken seamount (SO168-DR57-1) yield a statistically valid weighted mean age of 85.5 ± 3.3Ma (2σ, MSWD = 0.63, P = 0.64). The statistically valid inverse isochron age of 83.6 ± 2.6 Ma (95% conf.; MSWD = 1.9; P = 0.13; initial $^{40}Ar/^{36}Ar$ = 297.7 ± 2.1; but with a spreading factor value of only 22.0%, below the cut-off of > 40% suggested by Jourdan et al. (2009)) shows that these analyses preserved initial atmospheric $^{40}Ar/^{36}Ar$ ratios. The inverse isochron age, however, is within error of the weighted mean age. Nevertheless, the 5 analyses yield $^{36}Ar/^{37}Ar$ AI values above the plagioclase cut-off value of Baksi (2007) and elevated % $^{40}Ar_{atm}$ values indicate the degassing of Ar from altered material. Therefore the weighted mean age should be treated with caution. However, it should be noted that the SO168 DR57-1 plagioclase age of 85.5 ± 3.3 Ma (2σ) from East Chatham Rise lies within the age range of the seamounts from the nearby Hikurangi plateau (99-87 Ma; Hoernle et al., 2010), and the first magmatic phase of Chatham Island (85-82 Ma; Panter et al., 2006).

Table 1: $^{40}Ar/^{39}Ar$ results and calculated ages from Eastern Chatham Rise and Manihiki plateau.

Laser total fusion results								
Sample	**Location**	**Rock Type**	**Phase**	**Age (Ma)**	**2σ**	**MSWD**	**P**	**No. of analyses**
SO168 DR 57-1	Chicken	Trachyte	Plag.	85.5	±3.3	0.63	0.64	5 out of 16
Laser step-heating results								
Sample	**Location**	**Rock Type**	**Phase**	**Age (Ma)**	**2σ**	**MSWD**	**P**	**Cum. % ^{39}Ar**
SO193 DR 35-1	Smt. -DIT	Mugearite	Plag.	100.7	±0.93	1.6	0.18	61.9 %

Abbreviations: Plag. = plagioclase; Cum. = cumulative; MSWD = Mean Squares Weighted Deviation; P = probability; conf. = confidence; WMA = weighted mean age

3.2 Alteration and age correction of radiogenic isotope ratios

The evaluation of geochemical data from aged oceanic rocks needs to take into account the effect of seawater alteration. To minimize the effects of alteration, we sampled the freshest parts of the lavas by careful handpicking under a binocular microscope (size fraction 0.5-1mm). The loss on ignition (LOI), a common indicator for the degree of alteration, is relatively low (LOI < 3.3 wt. %) for these oceanic rocks (excluding 2 out of 19 samples with LOI values of 5.7 and 7.6 wt. %). In general, the HFSE, such as Zr, Nb, Ta and Hf, as well as the REE, are considered to be relatively immobile during low temperature seawater alteration, whereas the alkali elements, LILE and U are prone to low-temperature alteration and Pb to hydrothermal alteration (e.g. Hart, 1969; Hart et al., 1974; Thompson, 1983; Bienvenu et al., 1990; Verma, 1992; Jochum and Verma, 1996). Since our samples (with LOI < 3.3 wt.% and MgO > 2wt. %) have comparable correlation coefficients for immobile vs. immobile elements (e.g. Zr vs Nb, Th, Ba with the best fit line (R^2) values of 0.74-0.80; not shown) and immobile vs mobile elements (Zr vs Rb, K, Pb; R^2=0.73-0.86; not shown), we believe that our sample collection is relatively fresh. Accordingly, the major and incompatible multi-element diagrams show no evidence of seawater alteration through anomalous enrichment or depletion of the mobile elements irrespective of the LOI values (Figs. 2-4).

In order to compare the isotopic composition of rocks with different ages, we first calculate initial isotope ratios of samples based on their measured parent/daughter ratios (P/D) and then project these values to a common age of 60 Ma using source P/D values. Here, we use the proposed end member source compositions for HIMU (and EM I values for the basement lavas) after Stracke et al. (2003) and Willbold and Stracke (2006).

4. Results and HIMU geochemistry

In this section, we discuss the major and trace elements and isotopic variability of the HIMU reference locations and compare the geochemical compositions of our analyzed submarine samples to the compositions of the respective basement lavas and HIMU reference locations.

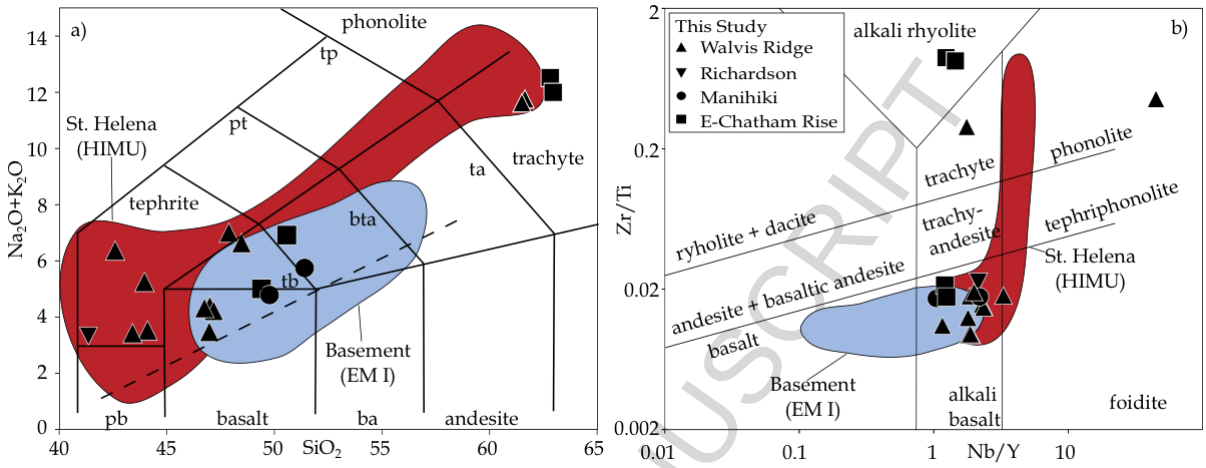

Fig. 2: Classification diagrams with a) SiO_2 vs total alkalis (Na_2O+K_2O) normalized to 100% on a volatile–free basis, after Le Maitre et al. (2005) and b) Nb/Y vs. Zr/Ti after Pearce (1996). The dashed line in a) divides the alkaline and sub-alkaline series, after MacDonald (1968). Basement (EM I) comprises the Richardson seamount, Manihiki Plateau and Walvis Ridge EM I-type basement lavas. Note, only EM I Gough-type composition is shown for the Walvis Ridge. The source of basement data is reported in Fig.1. St. Helena literature data: Baker, 1969; Grant et al., 1976; Weaver et al., 1987; Chaffey et al., 1989; Willbold and Stracke, 2006, 2010; Kawabata et al., 2011; Salters et al., 2011; Hanyu et al., 2014. Abbreviations: pb = picrobasalt, pt = phonotephrite, tp = tephriphonolite, tb = trachybasalt, bta = basaltic trachyandesite, ta = trachyandesite, ba = basaltic andesite.

[Two columns]

4.1 Major elements

Mafic lavas (MgO > 5wt.%) from the HIMU reference localities are alkalic and silica-undersaturated, characterized by low SiO_2 and Al_2O_3, but high CaO and total FeO (FeO^T) contents, and high CaO/Al_2O_3 ratios compared to other OIBs (Figs. 2-3; e.g.

Kogiso et al., 1998; Jackson and Dasgupta, 2008). While volatile-free peridotite or pure eclogite/pyroxenite (high pressure modification of MORB) cannot reproduce the major element characteristics of the HIMU end member lavas (e.g., Pertermann and Hirschmann, 2003; Kogiso and Hirschmann, 2006; Spandler et al., 2008; Dasgupta et al., 2010), experimental studies indicate that CO_2 is required in the mantle source to generate HIMU lavas (e.g., Dasgupta et al., 2007; Gerbode and Dasgupta, 2010; Mallik and Dasgupta, 2012, 2013). The involvement of CO_2 in the formation of silica-poor ocean island HIMU-type basalts is supported by phenocrysts with CO_2-rich inclusions (Cook-Austral: Saal et al., 1998; Weiss et al., 2011; Weiss et al., 2016). The characteristic major element composition of HIMU end member lavas is associated with the interaction (infiltration or metasomatism) of MORB-eclogite/pyroxenite derived melts and carbonated peridotite or a hybrid source, e.g. carbonated MORB-eclogite/pyroxenite derived melts added to peridotite (e.g., Dasgupta et al., 2007; Jackson and Dasgupta, 2008; Dasgupta et al., 2010; Gerbode and Dasgupta, 2010; Mallik and Dasgupta, 2012, 2013; Herzberg et al., 2014; Mallik and Dasgupta, 2014). Olivine phenocrysts with low Ni and high Ca contents, and low Fe/Mn ratios from HIMU lavas are consistent with peridotite as the dominate source lithology (Herzberg et al., 2014; Weiss et al., 2016), which became infiltrated/metasomatized by MORB-eclogite/pyroxenite derived melts (Herzberg et al., 2014) and/or carbonatitic fluids/melts (Weiss et al., 2016).

The volcanic rocks from the Walvis Ridge, Richardson, Eastern Chatham Rise/Hikurangi Plateau and Manihiki Plateau seamounts are also silica undersaturated, ranging from alkali basalts through trachytes to basanites through tephrites (Fig 2; Pearce, 1996; Le Maitre et al., 2005). On binary diagrams with MgO, the submarine samples (with LOI < 3.3 wt. %) form negative correlations with SiO_2, Al_2O_3, K_2O, Na_2O and positive correlations with CaO, FeO^T and TiO_2 (Fig. 3), consistent with fractional

crystallization of the observed phenocryst phases (olivine, clinopyroxene, feldspar and Fe-Ti oxides). The change in slope of the positive MgO versus CaO, SiO_2, FeO^T and TiO_2 trends at MgO values of ~ 5 wt. % indicates that clinopyroxene and Fe-Ti oxides become major fractionating phases at this stage of differentiation. P_2O_5 forms a similar trend as TiO_2 (not shown), indicating apatite fractionation at more evolved stages of differentiation (MgO < 4 wt. %). At a given MgO content (> 5 wt. %), the analyzed late-stage samples have distinct major element compositions trending to lower SiO_2 and higher FeO^T and TiO_2, compared to their respective EM I-type basement rocks (Fig. 3). The major element data for our samples lie within the compositional range of HIMU lavas from St. Helena and Cook-Austral islands (Fig. 3).

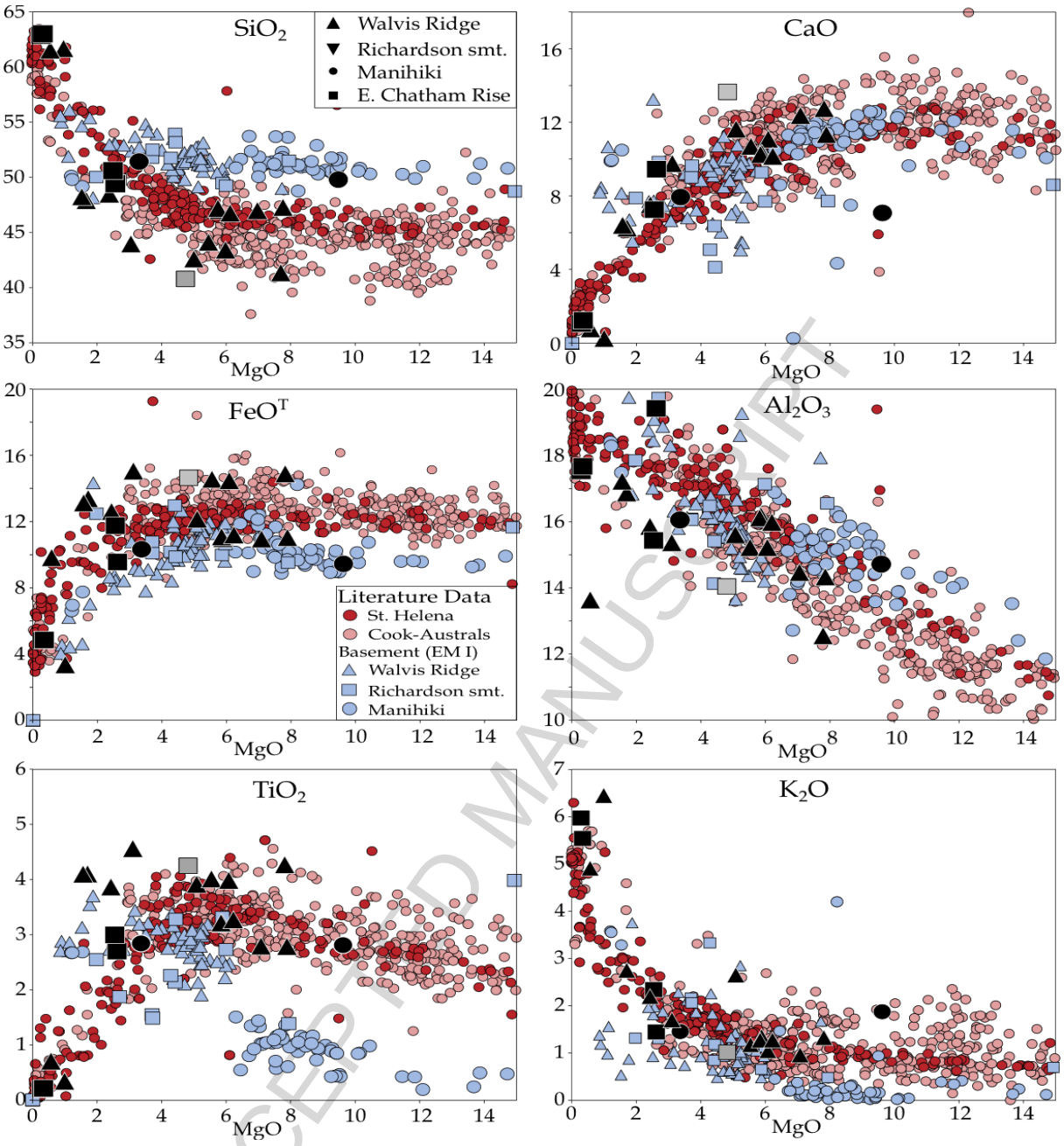

Fig. 3: Bivariate diagrams of MgO versus major elements with references from the EM-type basement lavas from the Manihiki plateau, Walvis Ridge and Richardson seamount, and St. Helena lavas and Cook-Austral island rocks for HIMU (Dupuy et al., 1989; Chauvel et al., 1992; Woodhead, 1996; Kogiso et al., 1997b; Lassiter et al., 2003; Hanyu et al., 2011; Salters et al., 2011; Hanyu et al., 2013; Maury et al., 2013). The gray rectangle (D35-1; Le Roex et al., 2010), which is also from a late-stage cone on Richardson Seamount, has a similar major element composition to our basanite sample from another late-stage cone on Richardson seamount. Major element oxides were normalized to 100% on a volatile-free basis. Literature data as in Fig.2.

[Two columns]

4.2 Trace elements

The HIMU reference localities have remarkably similar trace element compositions characterized by high primitive-mantle-normalized Nb and Ta concentrations relative to Ba, Th and Rb with decreasing normalized concentrations from Nb to Cs, and overall low Pb, Rb, and Ba concentrations relative to EM basalts (Fig. 4; Willbold and Stracke, 2006; Stracke, 2012). Willbold and Stracke (2006) pointed out that all HIMU basalts have low Ba/La, Rb/La, Rb/Sr and high U/Pb ratios compared to EM-type basalts, which is consistent with a source with lower (Rb, Ba, Th, U)/REE and Rb/Sr ratios and higher (U, Th)/Pb, Sm/Nd and Nb/La ratios compared to bulk Earth. The characteristic relative depletion of highly incompatible trace elements (e.g., Cs, Rb and Ba) and high (Nb, Ta)/(U, La) and Nd/Pb ratios could indicate a source, which is 1) depleted in highly incompatible elements and 2) additionally modified by loss of fluid-mobile elements (e.g., Chauvel et al., 1992; Woodhead, 1996; Stracke et al., 2003; Willbold and Stracke, 2006; Kawabata et al., 2011; Stracke, 2012). Stracke et al., 2003) showed that melting (~1%) of subduction-modified oceanic crust produces melts that broadly resemble those of HIMU basalts, even if the calculated melts have more pronounced positive Nb-Ta anomalies and higher Cs/Rb ratios (their Fig. 3). A critical aspect of the classic ocean-crust-recycling model remains that the overlying sediments are effectively removed from the subducting slab, since even small quantities would lead to radiogenic isotope ratios distinct from HIMU (e.g., Chauvel et al., 1992; Stracke et al., 2003). Alternatively, the HIMU multi-element pattern could reflect incompatible-element enrichment and depletion processes (e.g., Pilet et al., 2005; Castillo, 2015; Weiss et al., 2016). For example, Weiss et al. (2016) showed that depleted SCLM metasomatized by carbonatitic melts can reproduce the incompatible-element pattern

of Archean metasomtiszed mantle xenoliths (Grégoire et al., 2003) and average post-Archean SCLM (McDonough, 1990), which at low degrees of melting can produce HIMU-like multi-element patterns (their Fig. 2).

Our submarine samples also have distinct incompatible element abundances compared to the EM-type compositions of their basement lavas. As with reference HIMU, our seamount samples have greater enrichments in Nb and Ta relative to Rb, Ba, Th and LREEs, greater depletion in Pb relative to Ce and Nd, and depletion in Ti relative to Zr, Hf and Eu (Fig. 4). The seamount lavas have also higher incompatible element abundances (e.g., Ba, Th, U, Nb, Ta, and LREE; Fig. 4) and higher more to less incompatible element ratios, e.g. Nb/Yb (> 10), La/Yb (> 13), TiO_2/Yb (> 1) and Ti/V (> 150), indicating low degrees and/or deep melting of an enriched source. In contrast, the EM I-type basement lavas have lower Ti/Yb and (Th, Nb)/Yb ratios, pointing to shallower melting at higher degrees and/or a more depleted source composition. Finally, the late-stage seamount samples show the characteristic HIMU-pattern with overall increasing normalized concentrations from Lu to Nb-Ta, excluding relative Pb and K depletions, and then decreasing concentrations to Cs.

In summary, the late-stage seamount lavas have incompatible element patterns distinct from their EM I basement lavas, but similar to the St. Helena HIMU end member (Fig.4). The trace element characteristics of the HIMU-type late-stage magmas are consistent with being derived from (deep) low-degree melting of silica-undersaturated, carbonated pyroxenitic/ecologitic/peridotite source material (e.g., Weiss et al., 2011; Weiss et al., 2016).

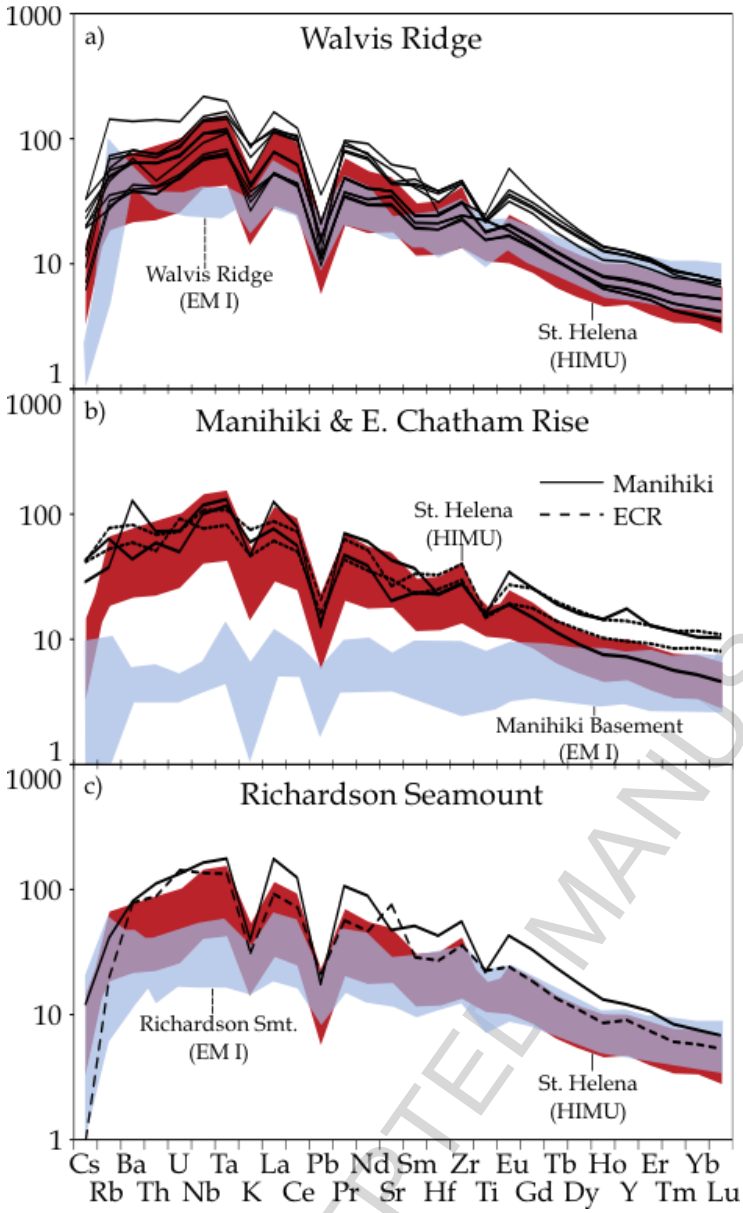

Fig. 4: Normalized incompatible element diagrams of a) late-stage volcanism on Walvis Ridge, b) late-stage volcanism on the Manihiki Plateau and volcanism on and adjacent to the Eastern Chatham Rise, and c) late-stage volcanism from the Richardson seamount in relation to the respective basement (blue) and St. Helena lavas (red). The element concentrations are normalized to primitive mantle after Hofmann (1988). Samples with MgO<2wt.% are not shown due to enhanced fractionation of accessory minerals that cause disturbance of element patterns. Note, the late-stage basanite sample (D35-1, dashed line in c) from the Richardson seamount, dated by O'Connor et al. (2012), also has a HIMU-like trace element composition (Le Roex et al., 2010), supporting a genetic and temporal association to the sample from the cone we studied (MSM19/3 DR6-1).

[One column]

4.3 Sr-Nd-Pb-Hf isotope data

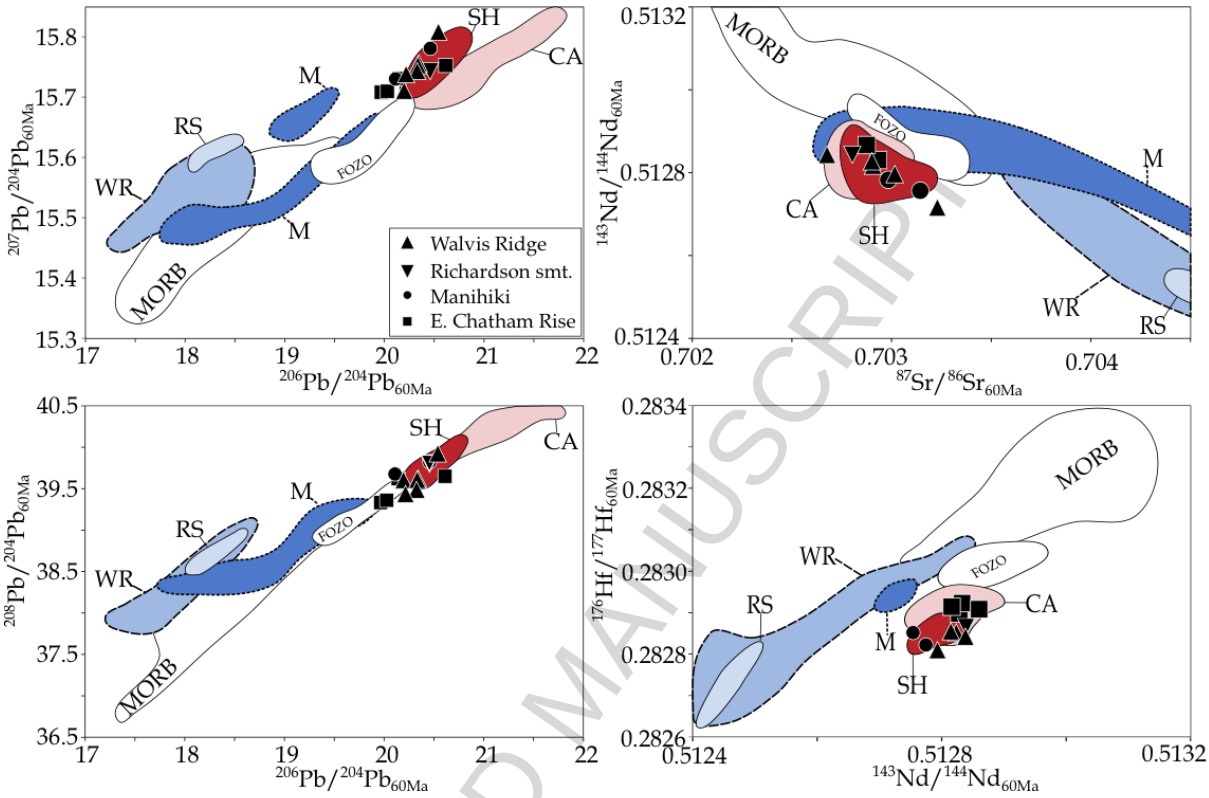

Fig. 5: Initial isotope ratios projected to 60 Ma using proposed source parent/daughter ratios for HIMU for the late-stage volcanism on and near the Walvis Ridge, Eastern Chatham Rise, Richardson Seamount, and the Manihiki Plateau. For comparison, fields for the respective basements are also shown, as well as Mid-Ocean Ridge Basalts (MORB), FOZO (Chauvel et al., 1992; Lassiter et al., 2003) as defined by Stracke et al. (2005), and end member HIMU reference locations, i.e. St. Helena and the Cook-Austral archipelago. Abbreviations: SH = St Helena, CA = Cook-Austral, M = Manihiki plateau, WR = Walvis Ridge, RS = Richardson seamount, MORB taken from the data compilation of Class, C. and Lehnert, K. (2012): PetDB Expert MORB (Mid-Ocean Ridge Basalt) Compilation.EarthChem Library. http://dx.doi.org/10.1594/IEDA/100060). The sources of other literature data are reported in Fig. 3. MORB values are corrected to 60Ma, assuming a depleted composition after Workman and Hart (2005).

[Two column]

The HIMU reference locations of St. Helena and Cook-Austral Islands have unique isotope ratios with $^{87}Sr/^{86}Sr_{60Ma}$ = 0.7023-0.7034, $^{143}Nd/^{144}Nd_{60Ma}$ = 0.5127-0.5129, $^{206}Pb/^{204}Pb_{60Ma}$ = 20.02-21.71, $^{207}Pb/^{204}Pb_{60Ma}$ = 15.65-15.84, $^{208}Pb/^{204}Pb_{60Ma}$ = 39.48-40.50 and $^{176}Hf/^{177}Hf_{60Ma}$ = 0.2828-0.2830 (Fig. 5). St. Helena and Cook-Austral lavas overlap in $^{206}Pb/^{204}Pb_{60Ma}$ vs. $^{208}Pb/^{204}Pb_{60Ma}$ and $^{87}Sr/^{86}Sr_{60Ma}$ vs. $^{143}Nd/^{144}Nd_{60Ma}$ isotope space, but the Cook-Austral Island lavas trend towards higher $^{206}Pb/^{204}Pb_{60Ma}$ and $^{208}Pb/^{204}Pb_{60Ma}$ ratios compared to St. Helena (Fig. 5). On the other hand, the St. Helena lavas are characterized by higher $^{207}Pb/^{204}Pb_{60Ma}$ at a given $^{206}Pb/^{204}Pb_{60Ma}$ value and slightly lower $^{176}Hf/^{177}Hf_{60Ma}$ at a given $^{143}Nd/^{144}Nd_{60Ma}$ value (Fig. 5). The variable $^{207}Pb/^{206}Pb$ ratios could reflect different formation ages, whereas the slightly lower $^{176}Hf/^{177}Hf_{60Ma}$ at a given $^{143}Nd/^{144}Nd_{60Ma}$ value could be generated by slightly lower Lu/Hf ratios (0.006 for 2 Ga radiogenic in-growth; Hanyu et al., 2014).

The analyzed samples have the following range in isotope ratios at 60 Ma: $^{87}Sr/^{86}Sr_{60Ma}$ = 0.7027-0.7032 (except SO168 DR58 with a $^{87}Sr/^{86}Sr_{60Ma}$ of 0.7053, most likely increased by seawater alteration), $^{143}Nd/^{144}Nd_{60Ma}$ = 0.5127-0.5129, $^{206}Pb/^{204}Pb_{60Ma}$ = 19.96-20.61, $^{207}Pb/^{204}Pb_{60Ma}$ = 15.71-15.82, $^{208}Pb/^{204}Pb_{60Ma}$ = 39.33-39.92 and $^{176}Hf/^{177}Hf_{60Ma}$ = 0.2827-0.2829, which overlap with the St. Helena HIMU composition in multi-isotope space (Fig. 5). In conclusion, the late-stage seamount samples have major and trace element and Sr-Nd-Pb-Hf isotopic compositions that overlap almost completely with the St. Helena HIMU end member composition (Fig. 5).

5. Worldwide distribution of HIMU

Late-stage volcanism on the Walvis Ridge (Tristan-Gough hotspot track), Richardson seamount (Shona hotspot track), Manihki Plateau and Eastern Chatham Rise/Hikurangi Plateau have distinct major and trace element and Sr-Nd-Pb-Hf isotopic compositions compared to their EM I-type basement rocks, but have similar

compositions to lavas from the end member HIMU island of St. Helena (Figs. 3-5). Our selected samples from the southern South Atlantic and the SW Pacific Ocean demonstrate that end member HIMU is not limited to St. Helena and Cook-Austral islands and may have an even wider distribution. Based on a broad literature survey, other samples with HIMU-type Sr-Nd-Pb isotopic and trace element compositions occur in oceanic and continental settings (Fig. 6).

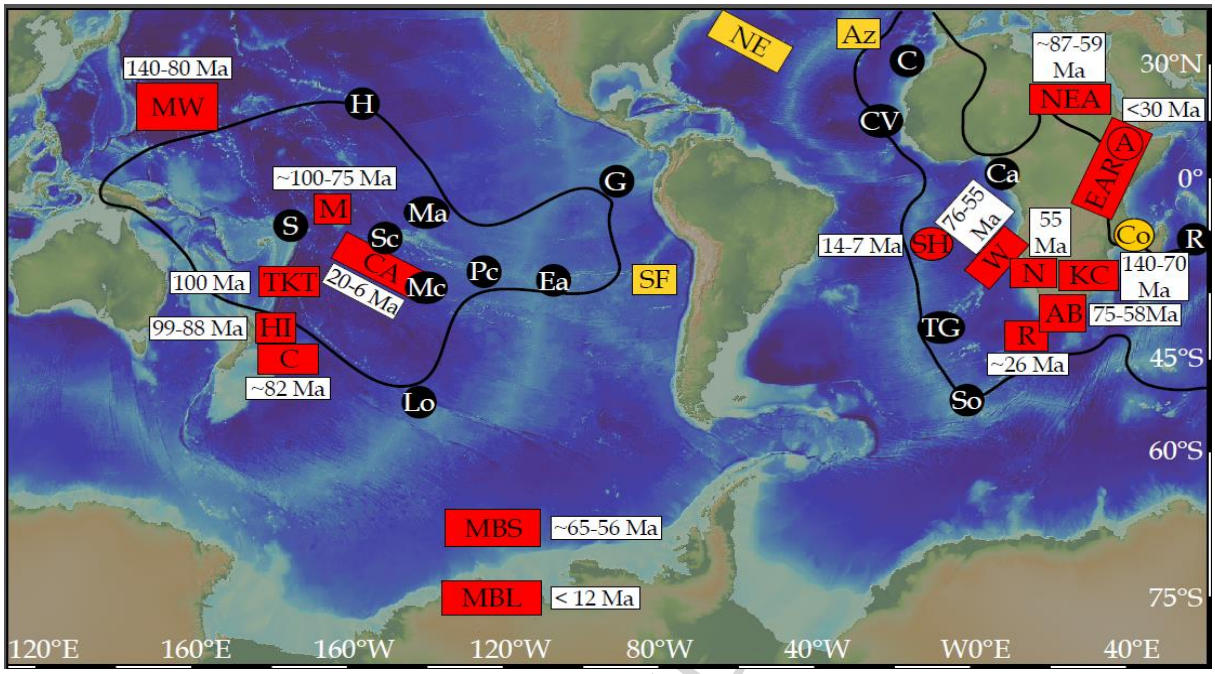

Fig. 6: Bathymetric map showing 1) the location of primary mantle plumes after French and Romanowicz (2015) and the proposed Shona hotspot (red circles denote present hotspots having HIMU compositions, and black circles show the locations of hotspots with non-HIMU isotopic compositions), 2) the 1% ∂V_s contour (black line) defining the Pacific and African large low shear velocity provinces (LLSVPs; Torsvik et al., 2010), 3) volcanic features with HIMU compositions (red rectangles) and their age ranges, and 4) locations with low Nd isotope ratios (LoNd) falling on the LoNd Array of Hart et al. (1986) (yellow). Abbreviations: Mantle plumes: H = Hawaii, S = Samoa, Sc = Society, Ma = Marqueses, Mc = Mcdonald, Pc = Pitcairn, Lo = Louisville, Ea = Easter, G = Galapagos, So = Shona, TG = Tristan and Gough, SH = St. Helena, Ca = Cameroon, CV = Cape Verde, C = Canary, A = Afar, Co = Comoros and R = Reunion; HIMU locations with age data: MW = Marshall and Wake seamount Group (Smith et al., 1989; Staudigel et al., 1991; Koppers et al., 1995; Koppers et al., 2003; Konter et al., 2008), CA = Cook-Austral islands (includes Mangaia, Tubuai and Old Rurutu volcanism), HI = Hikurangi Plateau, TKT = alkaline field near the Tonga-Kermadec Trench (Castillo et al., 2009), C = Chatham Island and Eastern Chatham Rise (this study), MBL= Marie Byrd Land (Hart et al., 1997; Panter et al., 2000), MBS = Marie Byrd Seamounts (Kipf et al., 2014), NEA = Northeast Africa (Sudan, Egypt; Lucassen et al., 2008), AB = Alphard Bank (Janney et al., 2002), EAR = East African Rift volcanics (carbonatites: Nelson et al., 1988; Kalt et al., 1997; Bell and Tilton, 2001 and silicates: Vollmer and Norry, 1983; Paslick et al., 1995; Simonetti and Bell, 1995; Stewart

and Rogers, 1996; Rogers et al., 2000; Roex et al., 2001; Furman et al., 2006; Keller et al., 2006; Mana et al., 2012), KC = Kaapvaal Craton kimberlites (Kramers, 1977; Collerson et al., 2010), N = Namibian carbonatites (Cooper and Reid, 1998; Cooper and Reid, 2000), W = Walvis Ridge (this study; Rohde et al., 2013b; O'Connor and Jokat, 2015a), R = Richardson Seamount of the Shona hotspot track (this study; O'Connor et al., 2012), M = Manihiki Plateau seamounts (this study); LoNd array (Hart et al., 1986): SF = San Felix and San Ambrosio, NE = New England Seamounts, AZ = Azores and Co = Comores. Source of map: http://www.geomapapp-org.

[Two columns]

5.1 Distribution of end member HIMU in the oceans

In addition to the localities for which we provide new data in this study, the oceanic settings where HIMU material was found comprise: the Cretaceous Marshall and Wake seamount group (140-80 Ma; e.g. Konter et al., 2008), late-stage volcanism on the Hikurangi plateau (99-88 Ma; Hoernle et al., 2010), alkalic lavas near the Tonga-Kermadec Trench in the western Pacific (100 Ma; Castillo et al., 2009), Paleocene Marie Byrd seamounts offshore Marie Byrd Land Antarctica (65-56 Ma; Kipf et al., 2014), Alphard Bank in the South Atlantic (~58 Ma, which represents an extension of the Western Cape Province in South Africa; Janney et al., 2002), and the two well-known reference localities, St. Helena (14-7 Ma; e.g. Chaffey et al., 1989; Hanyu et al., 2014) and Cook-Austral Islands (Fig. 6; 20-6 Ma; e.g. Woodhead, 1996; Chauvel et al., 1997; Hanyu et al., 2011).

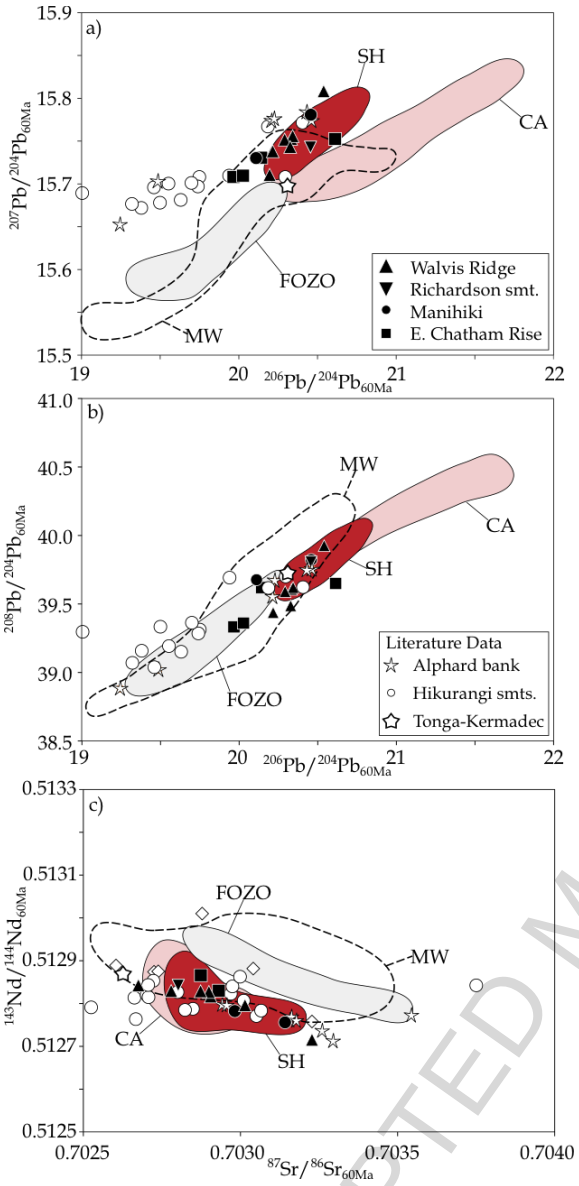

Fig. 7: HIMU locations in oceanic settings in multi-isotope space corrected to a common age of 60 Ma, which is the medium age of all reported HIMU localities. The isotope ratios of the respective locations overlap with HIMU from St. Helena. Abbreviations: SH = St. Helena, CA = Cook-Austral islands (includes Mangaia, Tubuai and Old Rurutu volcanism) and MW = Marshall-Wake seamount group. References for the respective sites are reported in Figs 5-6.

[One column]

In the oceanic intraplate settings, the most radiogenic samples (e.g. $^{206}Pb/^{204}Pb_{60Ma}$ ratios > 20.5) of the respective locations lie within the St. Helena HIMU composition on Sr-Nd-Pb isotope plots with the exception of the Marshall-Wake

seamount group, which also overlap the Cook-Austral HIMU field on the $^{206}Pb/^{204}Pb_{60Ma}$ and $^{207}Pb/^{204}Pb_{60Ma}$ diagram (Fig. 7). In general, the lavas from the Marshall-Wake seamount group (140-80 Ma) are the oldest submarine lavas on the seafloor with end member HIMU isotopic signature, and are therefore particularly prone to seawater alteration (e.g., elevated $^{87}Sr/^{86}Sr_{60Ma}$ ratios of several samples; Koppers et al., 2003; Konter et al., 2008). In addition, for the majority of samples, no comprehensive parent-daughter (e.g., U-Th-Pb) elemental concentration data sets are available; therefore, we had to estimate parent/daughter ratios. Since the Marshall-Wake seamounts are believed to represent the oldest submarine expression of the Cook-Austral hotspot system (Konter et al., 2008), we use the average trace element ratios of fresh Cook-Austral HIMU island basalts to calculate the initial isotope ratios. U and/or Pb depletion/enrichment could result in an over-/under-correction of the initial isotope ratios and in part explain the scatter of $^{208}Pb/^{204}Pb_{60Ma}$ at a given $^{206}Pb/^{204}Pb_{60Ma}$. However, even if the Marshall-Wake seamount group data spreads over a broader isotopic range at high $^{206}Pb/^{204}Pb_{60Ma}$ values, the compositional domain overlaps the HIMU end member composition in isotopic composition.

5.2 Distribution of end member HIMU on the continents

The continental localities of the HIMU end member include fragments of the Eastern Gondwana margin, including Cenozoic rift volcanics from Marie Byrd Land in the West Antarctic (<12 Ma; Hart et al., 1997) and Late Cretaceous volcanism on the Chatham Islands, New Zealand (85-82 Ma Panter et al., 2006), Cenozoic rift-related volcanism from the East African Rift (<30 Ma; e.g. Furman et al., 2006), intraplate volcanic rocks from North Africa (Sudan and Egypt; 87-59 Ma; Lucassen et al., 2008), Group I kimberlites from the Kaapvaal Craton, South Africa (140-70 Ma; e.g. Collerson et

al., 2010) and carbonatites from the Namaqua Natal Belt (Namibia; ~50 Ma; Cooper and Reid, 2000) and East African Rift (<130 Ma; e.g. Bell and Tilton, 2001; Fig. 6).

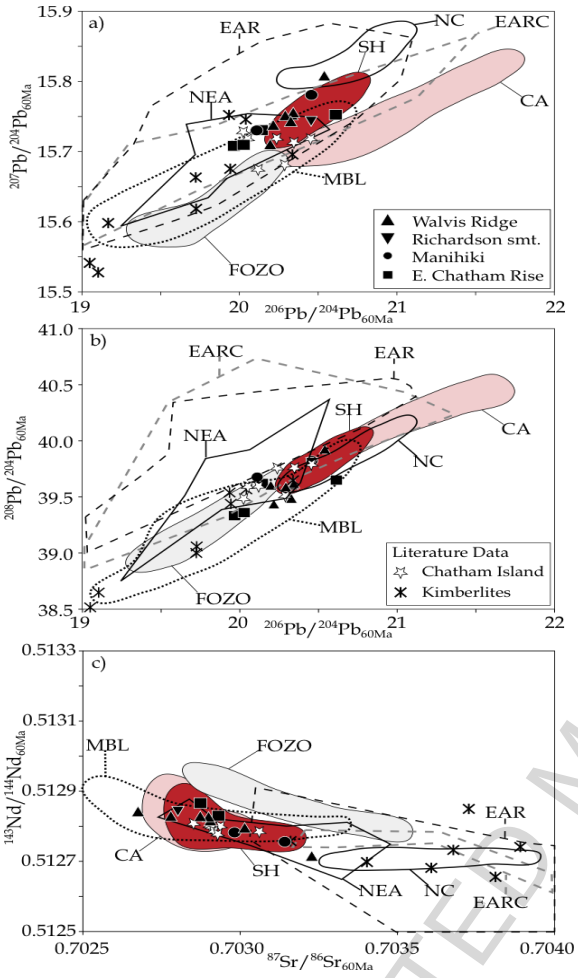

Fig. 8: Continental HIMU locations on different isotope correlation diagrams. Note, some of the continental settings (e.g., EAR) have lower Nd and Sr isotope ratios than HIMU, possibly reflecting crustal assimilation/contamination. Due to incomplete Sr-Nd-Pb isotope data from the Namibian carbonatites, averaged Sr and Nd isotope ratios from samples from the same volcanic complex were used to estimate the range of the Pb-Nd and Pb-Sr isotope fields. Note, the Hf isotope plots are not shown in Figs. 7-8, since the data have only been published from Marie Byrd, Alphard bank and the Group I Kimberlites. However, the Hf isotope data for these sample sites plot within the same range of St. Helena HIMU. Abbreviations: SH = St. Helena, CA = Cook-Austral islands (includes Mangaia, Tubuai and Old Rurutu volcanism), NC = Namibian carbonatites, EARC = East African Rift Carbonatites, MBL = Marie Byrd Land and seamounts, NEA = Northeast Africa and EAR = East African Rift silicates. The references for the respective sites are reported in Figs. 5-6.

[One column]

In contrast to most oceanic settings, the intraplate and rift-related continental volcanism spreads over a larger compositional range for the most radiogenic samples (e.g. $^{206}Pb/^{204}Pb_{60Ma}$ >20.5), but always include the HIMU composition (Fig. 8). The greater isotopic variation could reflects continental lithospheric interaction. The lavas with the most radiogenic Pb isotopic compositions (e.g. $^{206}Pb/^{204}Pb_{60Ma}$ > 20.5) from Chatham Island and Marie Byrd Land lie completely within the St. Helena compositional range in multi-isotope space (Fig. 8), demonstrating that the HIMU end member composition exists in continental settings (Hart et al., 1997; Panter et al., 2000; Panter et al., 2006). On the other hand, the East African Rift lavas (silicates and carbonatites) extend to more radiogenic $^{207}Pb/^{204}Pb_{60Ma}$ and $^{208}Pb/^{204}Pb_{60Ma}$ values, coupled with higher $^{87}Sr/^{86}Sr_{60Ma}$ and lower $^{143}Nd/^{144}Nd_{60Ma}$ ratios for a given $^{206}Pb/^{204}Pb_{60Ma}$ value in relation to St. Helena (Fig. 8). Although, it has been proposed that the silicate lavas and carbonatites are derived from the same source (Nelson et al., 1988; Bell, 2001; Bell and Tilton, 2001), the silicate lavas, compared to the carbonatites, show a considerably larger range in isotopic composition (higher $^{87}Sr/^{86}Sr_{60Ma}$, $^{207}Pb/^{204}Pb_{60Ma}$ and $^{208}Pb/^{204}Pb_{60Ma}$, but lower $^{143}Nd/^{144}Nd_{60Ma}$ ratios). This is consistent with greater amounts of crustal contamination affecting the silicate melts, which are generally hotter and have lower Sr, Nd and Pb concentrations than the carbonatitic lavas (~1000 ppm Sr on average in the silicate rocks compared to >5000 ppm in carbonatites, ~80 ppm Nd in silicates and up to 8000 ppm Nd in carbonatitites, and ~8 ppm Pb on average in silicates compared to 40 ppm in carbonatites) and thus are more susceptible to crustal contamination, whereas the high incompatible element concentrations in the carbonatites shield them from the effects of lithospheric interaction. Crustal contamination of the silicate melts is further supported by the inverse correlations of

silica content with $^{143}Nd/^{144}Nd$ and $^{206}Pb/^{204}Pb$ and positive correlation with $^{87}Sr/^{86}Sr$ isotope ratios for many of the silicate rocks suites (Fig. 8). The samples with the lowest silica contents have HIMU-like compositions ($^{143}Nd/^{144}Nd \sim 0.5127$, $^{206}Pb/^{204}Pb \sim 21$ and $^{87}Sr/^{86}Sr \sim 0.7035$), overlapping with the field for St. Helena HIMU (Mana et al., 2012). Alternatively, some of the trends formed by the data from the different locations may reflect mixing trends with EM I, as proposed for the isotopic array of East African carbonatites (Bell and Tilton, 2001).

In summary, volcanism with HIMU incompatible-element and isotopic characteristics has been identified between ~40°N and 80°S around the Earth, proving a near global distribution of HIMU (Fig. 6). Therefore, HIMU does not represent a rare, exotic composition, as previously proposed. Hart et al. (1986) proposed that intraplate volcanism in the Atlantic (St. Helena, New England Seamounts, Azores Islands and Walvis Ridge), Indian (Comoros Islands) and Pacific (Tubuaii, San Felix and San Ambrosio Islands) Oceans constitute a HIMU-EM I (or LoNd) mixing array and even Hawaiian and Samoan shield lavas show a trend towards a HIMU end member composition (e.g., Ren et al., 2009; Jackson et al., 2010; Jackson et al., 2014), which suggests that HIMU could be even more widespread in the sources of oceanic intraplate volcanism than just the end member localities noted above (Fig. 6).

6. Shallow or deep HIMU reservoir(s)?

A fundamental question that needs to be addressed is the location of the HIMU reservoir(s) within the Earth. Considering the restricted incompatible-element composition and isotopic characteristics of HIMU lavas, they are likely to be genetically related and have evolved from sources with a reasonably uniform composition under similar conditions, over similar time periods (Stracke et al., 2003; Stracke et al., 2005; Hanyu et al., 2014; Kimura et al., 2016). The radiogenic Pb isotope ratios of HIMU

require long-time isolation of 1-3.2 Ga (e.g. Tatsumoto, 1978; Zindler and Hart, 1986; Kawabata et al., 2011; Nebel et al., 2013; Hanyu et al., 2014; Castillo, 2015; Kimura et al., 2016). Fluid dynamic experiments and mantle convection models indicate that substantial mantle heterogeneities should be homogenized within less than 1 Ga in the convective mantle (e.g. Hoffman and McKenzie, 1985; Kellogg and Turcotte, 1990; Allègre et al., 1995; van Keken et al., 2002; Coltice and Schmalzl, 2006). Therefore, the convective upper mantle and even most of the lower convective mantle, where mixing could be more sluggish and hampered by phase changes, cannot preserve large-scale heterogeneities over the age of the Earth (van Keken et al., 2002).

Two potential regions exist within Earth where end member HIMU could be isolated from the convecting mantle since the Archean to Early Proterozoic: 1) shallow subcontinental lithospheric mantle (SCLM) reservoir (e.g., Stein et al., 1997; Lucassen et al., 2008; Rooney et al., 2014), or 2) deep reservoir at the base of the lower mantle (e.g., Hofmann and White, 1982; Chauvel et al., 1992; Stracke et al., 2005; Hanyu et al., 2014; Weiss et al., 2016). Several lines of evidence favor derivation from a deep reservoir, as described below. To begin with, the two end member HIMU-type localities are part of age-progressive volcanic chains consistent with derivation from deep mantle plumes (e.g., Chaffey et al., 1989; Chauvel et al., 1992; O'Connor et al., 2012; Hanyu et al., 2014). A deep origin for these plumes is further supported by seismic tomography, which has imaged low seismic velocity anomalies beneath these hotspot tracks down to the lowermost mantle (e.g. Montelli et al., 2006; French and Romanowicz, 2015). Using geochemical and geophysical constraints, Jackson et al. (2018) argue that there is a strong association of the extreme HIMU signature ($^{206}Pb/^{204}Pb > 20$) with deep-rooted mantle plumes.

The other oceanic HIMU settings can also be related to hotspot volcanism, e.g., the Walvis Ridge is related to the Tristan-Gough hotspot track (e.g., Richardson et al., 1982; Rohde et al., 2013b; Hoernle et al., 2015; O'Connor and Jokat, 2015a), the Richardson seamount to the Shona hotspot track (O'Connor et al., 2012; Hoernle et al., 2016) and the Marshall-Wake seamount group to the Austral-Cook hotspot system (Konter et al., 2008). The Ontong Java, Hikurangi and Manihiki plateaus are believed to have formed from a single massive upwelling from the lower mantle at ~120-125 Ma (e.g., Taylor, 2006; Hoernle et al., 2010; Timm et al., 2011; Hochmuth et al., 2015; Golowin et al., 2017). Note that our selected samples from the Walvis Ridge, Richardson Seamount, Hikurangi Plateau and Manihiki Plateau all represent late-stage volcanism, and apart from the Manihiki Plateau (Timm et al., 2011; Golowin et al., 2017), the respective EM I-type basements show no evidence of a HIMU signature. Therefore, it is unlikely that the late-stage Walvis, Shona and Hikurangi lavas are directly related to the mantle plumes forming the major morphological seafloor anomaly.

Carbonatites are commonly associated with mantle plumes (Nelson et al., 1988; Bell, 2001; Hoernle et al., 2002), e.g., East African Rift carbonatites and low-silica igneous rocks are related to the Afar mantle plume (Nelson et al., 1988; Bell, 2001; Bell and Tilton, 2001), whereas Canary and Cape Verde carbonatites are related to the mantle plumes forming the archipelagoes (Hoernle et al., 1991; Hoernle et al., 2002). In general, high pressure mineral phases in diamonds (e.g., Kaminsky, 2012) and primitive noble gas signatures (Sumino et al., 2006) point to a lower mantle origin for Group I kimberlites. Torsvik et al. (2010) calculated that the eruptive sites of ~80% (1112 out of 1395) of the kimberlite eruptions over the past 320 Ma lay close to the "plume generation zones" at the margins of the large low shear velocity provinces (LLSVPs) at the base of the lower mantle, and thus assume a similar source region for kimberlite

magmas as postulated for mantle plumes. Experimental studies show that a continuous series from carbonatite to kimberlite and silica-undersaturated melts can be generated by increasing degrees of melting of carbonated peridotite (e.g., Dalton and Presnall, 1998; Moore and Wood, 1998; Gudfinnsson and Presnall, 2005; Dasgupta et al., 2007), indicating that they are also genetically related and may ultimately be derived from a common source (Nelson et al., 1988; Bell, 2001; Nowell et al., 2004).

It has been proposed that the HIMU signature at the Eastern Gondwana margin (EGM; including West Antarctica and Zealandia) was derived from continental lithosphere previously metasomatized by a plume with a HIMU composition that may have triggered the break-away of Zealandia from Antarctica (e.g. Weaver et al., 1994; Storey et al., 1999; Hoernle et al., 2010; Kipf et al., 2014). $^{238}U/^{206}Pb$ and $^{232}Th/^{208}Pb$ error chron ages for mantle xenoliths from various localities within Zealandia consistently indicate that this metasomatic event is young and occurred within the last ~120 Ma from melts that already carried a HIMU signature (McCoy-West et al., 2016). Tectonic reconstructions at 100 Ma show an elongate belt of volcanic rocks with HIMU-like Pb isotopic compositions at the boundary between parts of Zealandia and Marie Byrd Land (Finn et al., 2005), consistent with a HIMU plume initiating the break-up of Zealandia from West-Antarctica (Weaver et al., 1994; Hart et al., 1997; Storey et al., 1999; Panter et al., 2000; Panter et al., 2006; Hoernle et al., 2010; Kipf et al., 2014; McCoy-West et al., 2016). Likewise, Kipf et al. (2014) and Hart et al. (1997) proposed that the HIMU source beneath the Marie Byrd Seamounts and Marie Byrd Land represent fossilized HIMU mantle plume material preserved at the base of the western Antarctic lithosphere, which was melted by decompression caused by continental edge convection and extension related to the initiation of the West Antarctic rift system respectively.

In summary, most HIMU locations appear to be related to mantle plumes derived from the Pacific and African LLSVP´s or their margins (e.g., Torsvik et al., 2006; Burke et al., 2008; Steinberger and Torsvik, 2012; French and Romanowicz, 2015). Therefore, the HIMU source material is also likely to derived from the LLSVP´s or be stored as a layer on the LLSVPs.

7. HIMU reservoir formation in an Archean geodynamical context

7.1 Age of the HIMU reservoir formation

Now we will discuss the timing and mechanism of HIMU reservoir formation in the context to the geodynamic setting under which HIMU may have originated. Based on Pb model ages, the proposed HIMU reservoir formation ages range between 1 and 3.2 Ga (Tatsumoto, 1978; Hofmann, 1997; Stracke et al., 2005; Hanyu et al., 2011; Nebel et al., 2013; Castillo, 2015). Recently, Kimura et al. (2016) proposed a *minimum* reservoir formation age range for HIMU of 2.0-2.5 Ga by numerical simulation of the source evolution and mixing relationships of EM I and HIMU. Based on negative $\Delta^{33}S$ ratios preserved in olivines from Cook-Austral HIMU lavas, Cabral et al. (2013) proposed that their source must be ≥ 2.45 Ga. As shown earlier (section 4.3; Fig. 5), the Atlantic HIMU end member has higher $^{207}Pb/^{204}Pb$ ratios at a given $^{206}Pb/^{204}Pb$ ratio compared to the Cook-Austral HIMU signature, which can be explained by an ~0.3 Ga older age of the St. Helena HIMU source (Hanyu et al., 2014). Since our new data and almost all other HIMU localities from the literature overlap with St. Helena (excluding Marshall and Wake seamount groups, which overlap with Cook-Austral HIMU) in Pb isotope space (Fig. 8), most HIMU is likely to have formed at ≥2.75 Ga (Neoarchean) and possibly even in the Meso- to Paleoarchean (e.g., Nebel et al., 2013). Finally, Archean HIMU-like lavas have been found in western Australia and India, indicating that the HIMU source has existed at least since 2.7 Ga (Said and Kerrich (2010) Manikyamba and Kerrich (2011).

In general, the composition of HIMU is directly related to mantle reservoirs that underwent temporal variations (e.g., isotopic composition of MORB or DM; Salters and Stracke, 2004; Stracke et al., 2005), and it has been proposed that the restricted geochemical signature of HIMU (compared to other end members) could reflect a short time interval for reservoir formation (Stracke et al., 2005; Willbold and Stracke, 2006; Kimura et al., 2016). Interestingly, the assumed minimum age of St. Helena HIMU coincides with the peak of episodic continental crust growth at ~2.7 Ga (e.g. McCulloch and Bennett, 1994; Stein and Hofmann, 1994; Condie, 2000; Rino et al., 2004; O'Neill et al., 2007). High continental crustal growth rates are associated with massive crustal production, as well as with increased recycling rates (Condie, 2000). During such an event a widespread HIMU reservoir(s) could have formed within a discrete age interval. Alternatively, the proposed HIMU reservoir formation ages could reflect the average age of accumulated packages of recycled material (Hanyu et al., 2014). This implies that the mechanism (recycling style) of the formation of the HIMU reservoir must have been stable over a certain time interval in the Neo- to Paleoarchean.

7.2 The style of Archean tectonics

Now we will discuss the geodynamic setting for an Archean HIMU reservoir formation age. In general, the tectonic style of the Archean earth and thus the recycling mechanism remains a matter of considerable controversy (Foley et al., 2003; Bédard, 2006; Van Kranendonk, 2010; Gerya, 2014; Harris and Bédard, 2014; Moyen and Laurent, 2018), but it has been suggested that the Early Archean Earth and its tectonic style were comparable to present-day plume-lid tectonics on Venus. Plume-lid tectonics is mainly driven by mantle up- and down-wellings (e.g., Van Kranendonk, 2010; Gerya, 2014; Harris and Bédard, 2014; Gerya et al., 2015).

How modern-style plate tectonics (defined by self-induced plate movement with passive mantle up-wellings beneath mid-ocean ridges and "stable" subduction zones, where the slabs sink deep into the mantle) initiated is still a matter of debate, but the global geodynamic regime most likely evolved gradually from plume-lid tectonics into modern-style subduction between 3.2 - 2.5 Ga (e.g., Condie and Kröner, 2008; Shirey and Richardson, 2011; Gerya, 2014; Moyen and Laurent, 2018). The driving recycling mechanism in the overall hotter mantle with Venus-like active-stagnant-lid regime was dominated by drip tectonics (lithospheric delamination), whereas subduction was a subordinate process (Bédard, 2006; Condie and Kröner, 2008; Gerya, 2014; Herzberg, 2014; Johnson et al., 2014). During the transition from plume-lid to modern-style tectonics, subduction was most likely flat and unstable (subducting crust was hotter and subduction angles were flatter; e.g., Karsten et al., 1996), with slab break-off being more frequent compared to present day subduction (e.g., Gerya, 2014; Bédard, 2018; Moyen and Laurent, 2018).

In summary, based on the age constraints described above (section 7.1), the minimum St. Helena HIMU reservoir formation age is likely to be ~2.75 Ga, but Meso- to Paleoarchean reservoir formation ages are also possible (Nebel et al., 2013). Therefore, it seems unlikely that that the classic end member HIMU reservoir formed as a result of modern-style tectonics. Below we discuss the possibility of classic HIMU forming in an Archean geodynamic context.

7.3 An alternative model for the HIMU reservoir formation in the Archean tectonic system

In the following section, we describe a concept for the generation of a widespread HIMU reservoir(s) in an Archean geodynamic setting before modern-style tectonics became established and formed the dominant recycling mechanism. Several

observations are inconsistent with the formation of reference HIMU through recycling of ocean crust: 1) major element and melt inclusion evidence that peridotite rather than eclogite/pyroxenit represents the dominate source lithology, 2) the isotopic compostion of HIMU does not lie on the extension of the MORB array, precluding a simple link between MORB and reference HIMU, and 3) in the Archean (at >2.45 Ga) drip tectonics (lithospheric delamination) rather than modern-day tectonics (with the deep subduction of oceanic lithosphere) was the dominant tectonic style. Therefore, oceanic lithosphere recycled through the lower mantle is unlikely to have generated a widespread Archean HIMU reservoir(s). Therefore, we favor an alternative model, which invokes shallow subduction and carbonatitic metasomatism of SCLM followed by delamination of the metasomatized SCLM into the lower mantle, similar to the model of Weiss et al. (2016).

Table 2: Estimates of the dehydration of subducted oeanic crust and metasomatized SCLM

	Rb	**Sr**	**Sm**	**Nd**	**Lu**	**Hf**	**U**	**Pb**
Bulk ocean crust (ppm)	2.99	136	3.11	9.55	0.45	2.28	0.115	0.48
Mobility (%)	0.630	0.410	0.140	0.310	0.010	0.220	0.290	0.850
Ca-rich sediment (ppm)	14.45	955	3.30	14.37	0.326	1.25	1.45	11.68
Mobility Melt-Sed. (%)	0.340	0.460	0.200	0.210	0.200	0.450	0.310	0.130
Total release (ppm)	6.80	495	1.10	5.98	0.070	1.07	0.483	1.93
DM (ppm)	0.088	9.800	0.270	0.713	0.063	0.199	0.005	0.023

	Rb/Sr		**Sm/Nd**		**Lu/Hf**		**U/Pb**	
% of metasomatism	1%	5%	1%	5%	1%	5%	1%	5%
Metasomatized SCLM (ppm)	0.011	0.012	0.363	0.319	0.304	0.261	0.225	0.242

HIMU reservoir formation Age	**Rb/Sr**		**Sm/Nd**		**Lu/Hf**		**U/Pb**	
	min.	max.	min.	max.	min.	max.	min.	max.
2.5 - 3.5 Ga (ppm)	0.009	0.020	0.339	0.364	0.237	0.265	0.168	0.256

Composition of bulk oceanic crust taken from Stracke et al. (2003); mobility estimates of ocean crust dehydration are taken from Kogiso et al. (1997a); Ca-rich sediment composition is the average composition of Ca-rich sediments from Plank and Langmuir (1998); mobility estimates for melt sediment

exchange at 900°C are derived according to the parameters given by Johnson and Plank (2000); DM composition after Salters and Stracke (2004), the required Rb/Sr, Sm/Nd, Lu/Hf and U/Pb ratios to produce HIMU within 2.5-3.5 Ga were calculated using the model of Stracke et al. (2003) with a HIMU compositional range of: $^{87}Sr/^{86}Sr$= 0.7027-0.7033, $^{143}Nd/^{144}Nd$= 0.5128-0 5130, $^{176}Hf/^{177}H$= 0.2828-0.2830,$^{206}Pb/^{204}Pb$= 20 - 22

The marine carbonate recycling hypothesis of Castillo (2015) invokes the recycling of Archean marine carbonates (a few %) and mixing with a depleted mantle component (oceanic lithospheric mantle) involving recycling of ocean lithosphere in the context of modern-style tectonics. Based on high U/Pb ratios (and thus high μ values of > 30 values), relatively low Ƙ ($^{232}Th/^{238}U$) and low Rb/Sr ratios (~0.005) in marine carbonates, Castillo (2015) showed that a mixture of Archean marine carbonates and depleted (oceanic lithospheric) mantle could evolve the characteristic $^{206}Pb/^{204}Pb$, $^{207}Pb/^{204}Pb$, $^{208}Pb/^{204}Pb$ and $^{87}Sr/^{86}Sr$ ratios of HIMU in ≥ 2.5 Ga, whereas the ancient depleted component controls the radiogenic $^{143}Nd/^{144}Nd$ and $^{177}Hf/^{176}Hf$ isotope ratios.

Finding low Ni contents and high Mn/Fe and Ca/Al ratios in olivines from HIMU lavas, Weiss et al. (2016) argued that Early Proterozoic/Archean subducting slabs released fluids/melts with carbonatitic affinity that metasomatized the overlying melt-depleted peridotitic SCLM. A role for carbonatitic metasomatism is also supported by high CaO contents and carbonate-rich inclusions in HIMU olivine phenocrysts (Saal et al., 1998; Weiss et al., 2011; Weiss et al., 2016). Under this scenario, the incompatible-element signature of Archean marine carbonates (high U/Pb and low Th/U and Rb/Sr ratios) is imprinted on the depleted SCLM. As mentioned above (section 4.2), such a source can produce HIMU-like incompatible-element patterns at low degrees of melting (Weiss et al., 2016). In order to calculate the composition of fluids generated through the dehydration of subducting oceanic crust and carbonate-rich marine sediments (with a

composition after Plank and Langmuir, 1998), we used the model of Stracke et al. (2003). Mixing this metasomatic agent with 95-99% DM (Salters and Stracke, 2004) forms parent-daughter ratios that can generate HIMU isotopic compositions within 2.5-3.5 Ga (Table 2).

As mentioned above, a carbonated peridotite or hybrid (peridotite + eclogite/pyroxenite) source lithology is required to account for the major element systematics observed in HIMU lavas. Hanyu et al. (2011) proposed that the Re-Os systematics of HIMU lavas provide a timing of the peridotite + carbonated eclogite/pyroxenite connection. Radiogenic $^{187}Os/^{188}Os$ ratios are derived from a source with high time-integrated Re/Os ratios, reflecting an ancient crustal source. HIMU lavas have radiogenic $^{187}Os/^{188}Os$ ratios (0.14-15), irrespective of the Pb and Hf isotope ratios (e.g., Schiano et al., 2001; Hanyu et al., 2011). These ratios show that mixing of pure recycled and long-term isolated oceanic crust within the mantle cannot reproduce the observed Os-Pb-Hf systematics. An early (before formation of the HIMU reservoir) and significant elevation of the Os concentration is required to lower the HIMU reservoir $^{187}Os/^{188}Os$ ratios to the presently observed values. Hanyu et al. (2011) propose that partial melts form recycled oceanic crust reacts with mantle material (with high Os concentrations) before the HIMU source was isolated, which is in agreement with the proposed carbonatitic metasomatism model of Weiss et al. (2016).

This model is also in accordance with the Archean geodynamic regime, i.e. plume-lid tectonics, where only small amounts of oceanic crust would be subducted to shallow mantle depths before subduction ceased and shifted to another location (Jacob and Foley, 1999; Foley et al., 2003). Accordingly, this would result in the formation of more widespread metasomatized SCLM, in contrast to modern-style tectonics where subduction zones are more stable and thus stationary over long periods of time (up to

several hundred million years), and are also steeper and thus more locally focused. It has been suggested that metasomatism contributes to the destabilization, i.e. detachment/delamination of SCLM, into the mantle compared to unmetasomatized SCLM (e.g., Foley et al., 2003; Lee, 2006; Krystopowicz and Currie, 2013). Finally, carbonate supersaturation of Archean seawater and precipitation of Ca-rich phases on the seafloor, as well as accompanying reactions with the oceanic crust (Sumner and Grotzinger, 1996; Higgins et al., 2009), could account for enhanced carbonation of the "oceanic crust". Enhanced carbonation of the seafloor could result in predominantly carbonatitic metasomatism of the overlying lithosphere during relatively flat subduction.

Destabilization resulting in detachment/delamination of carbonatite-metasomatized SCLM in the Archean before or during the transition from plume-lid to modern-style tectonics could be a suitable process for transferring geochemically enriched SCLM to the base of the lower mantle (Fig 9). Detachment/delamination is also likely to have increased during major intervals of crustal growth, such as at ~2.75 Ga (e.g., Hofmann et al., 1986; Condie, 2000). Storage for ≥2.5 Ga before recycling to the surface by mantle plumes could allow such metasomatized material to develop a HIMU composition. One major advantage of this hypothesis, in contrast to the ocean-crust recycling model, is that the HIMU reservoir is not strictly limited to the lowermost mantle (Fig. 9). Smaller batches of carbonate-metasomatised SCLM could continue to reside beneath Archean Cratons where they can contribute to shallow, rift-related melting or be delaminated during younger continental breakup events and recycled through the shallow (e.g., Hanan et al., 2004; Kipf et al., 2014; Hoernle et al., 2016), and/or deep mantle. Therefore not all HIMU has to be associated with deep mantle plumes, although much of it appears to be.

Most OIBs and MORBs with HIMU-like characteristics require a mixing end member with radiogenic Pb isotopic composition that is distinct from the classic HIMU end member (Stracke et al., 2005), characterized by more radiogenic $^{87}Sr/^{86}Sr$ and $^{208}Pb/^{204}Pb$ at a given $^{206}Pb/^{204}Pb$ isotope ratio (FOZO end member). The formation of FOZO (also termed "Young HIMU"; Thirlwall, 1997) is usually explained by a similar mechanism, but with overall younger formation ages compared to HIMU (e.g., Thirlwall, 1997; Stracke et al., 2005; Castillo, 2015). In contrast to HIMU, FOZO lies at the enriched end on the MORB array in multi-isotope space (Fig. 5; Stracke et al., 2005; Castillo, 2015), which suggests a close genetic relationship between FOZO and MORB. Since modern-style tectonics is likely to have been established since the Archean to Proterozoic transition, recycling of oceanic crust/lithosphere could be a potential source of FOZO (e.g., Hanan and Graham, 1996; Stracke et al., 2003; Stracke et al., 2005; Kimura et al., 2016).

In contrast to HIMU, which always has low $^{3}He/^{4}He$ ratios (lower than MORB; e.g., Kurz et al., 1982; Graham et al., 1992), some lavas with FOZO type (HIMU-like) composition have high $^{3}He/^{4}He$ ratios. Since the $^{3}He/^{4}He$ ratio of the depleted mantle may have decreased over time (Class and Goldstein, 2005; Jackson et al., 2008), high $^{3}He/^{4}He$ ratios (> 9 R/Ra) in some FOZO-like lavas could reflect ancient oceanic lithosphere, which became a closed system due to phase transformation (cf., Jackson et al., 2008; Castillo, 2015). In contrast, FOZO-like lavas with lower $^{3}He/^{4}He$ ratios could be derived from younger recycled oceanic lithosphere and/or sources with higher U and Th concentrations that would produce greater amounts of radiogenic ^{4}He. Therefore, the HIMU and FOZO (HIMU-like) end members are likely to be derived from different sources over different lengths of time. The change from Archean style drip tectonics, associated with carbonatitic metasomatism of SCLM, to modern style tectonics, in which

ocean lithosphere is recycled through subduction and mantle plumes, is a possible mechanism that can explain the distinct isotope ratios of HIMU and FOZO.

In summary, we propose that the classic HIMU end member is derived from carbonate metasomatized SCLM that is recycled through the lower mantle via detachment/delamination and returned to the surface via mantle plumes during plume-lid tectonics taking place in the Archean. During modern-style subduction in the Proterozoic, HIMU-like (or FOZO type) ocean island basalts are formed through the recycling of ocean crust through the lower mantle.

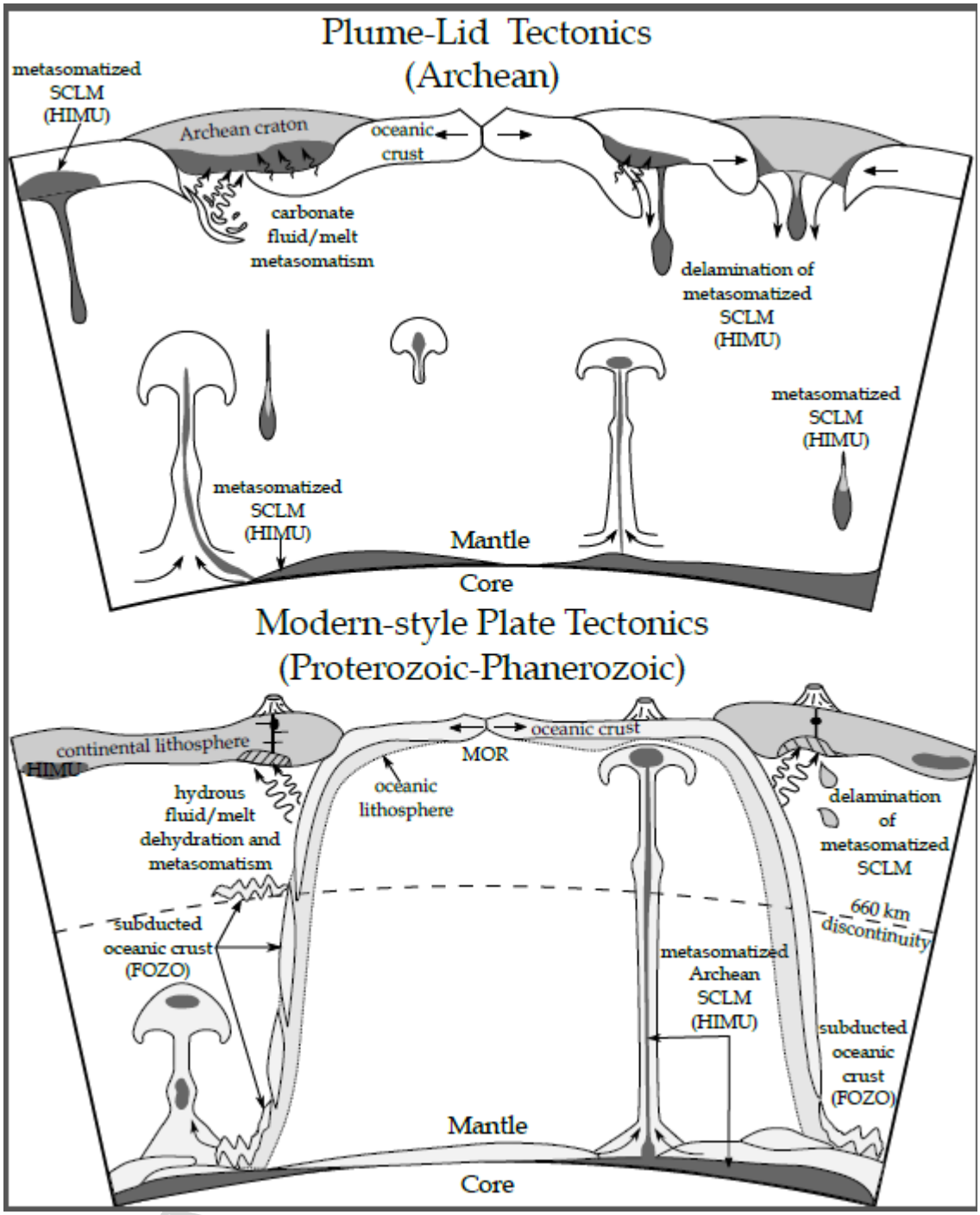

Fig. 9: Schematic models for the formation of the HIMU and FOZO end member reservoirs in the mantle. A) In the Archean, flat subduction was an integral part of plume-lid tectonics. Decarbonation of the shallowly subducting oceanic lithosphere caused metasomatism of the subcontinental lithospheric mantle (SCLM) by carbonate-rich fluids/melts, which also destabilized the SCLM. Drip tectonics and subduction suction resulted in detachment/delamination of the SCLM to the base of the mantle. The carbonate-metasomatized SCLM had high U/Pb and low Th/U and

Rb/Sr ratios that over time generated end member HIMU isotopic composition. B) Beginning roughly at the Archean-Proterozoic boundary, modern-style tectonics led to the subduction of oceanic lithosphere to the base of the lower mantle. The hydrothermally altered (shortly after formation at a mid-ocean ridge) and subsequently dehydrated (during shallow subduction) ocean crust had high U/Pb and slightly higher Th/U and Rb/Sr than the carbonate-metasomatized SCLM that generated HIMU. Over time the subducted crust stored at a thermal boundary layer such as the core-boundary and possibly upper-lower mantle boundary generated HIMU-like (FOZO) type compositions. Mantle plumes sample the delaminated Archean HIMU and the subducted ocean crust (FOZO) stored at the base of the lower mantle.

[One column]

8. Conclusions

This study evaluates the distribution and origin of the HIMU end member. Our new data from late-stage volcanic edifices on the Walvis Ridge and Richardson Seamount in the South Atlantic Ocean and from the Eastern Chatham Rise and Manihiki Plateau in the Western Pacific Ocean, combined with a literature data survey, show that the HIMU end member is likely to be globally distributed and present in oceanic and continental intraplate and rift-type settings. Rock types with HIMU compositions include carbonatites, Group I kimberlites and silica-undersaturated lavas (e.g., melilitites, nephelinites and basanites and related differentiated rocks), which generally represent low-volume melts. Most HIMU end member volcanism is apparently related to deep-seated mantle plumes, as indicated by seismic tomography at HIMU-type localities. The HIMU reservoir primarily formed in the Archean (≥2.5 Ga), which was dominated by drip tectonics (lithospheric detachment/delamination). Subduction of oceanic lithosphere was a subordinate process and only occurred to shallow depths. Drip tectonics provides a mechanism for transferring carbonate-metasomatized SCLM (Weiss et al. (2016) into the lower mantle. During the Proterozoic-Phanerozoic, modern-style plate tectonics dominated, characterized by dehydration of subducted crust at shallow depths and subsequent recycling of oceanic lithosphere through the lower mantle. Hydrothermal alteration of the ocean crust shortly after formation and dehydration during shallow subduction gives the ocean crust the appropriate composition to evolve HIMU-like (FOZO-type) compositions, which lie on an extension of the MORB array. Therefore our model invokes a different origin for the HIMU (through carbonate metasomatism and detachment/delamination of SCLM during Archean plume-lid tectonics) and FOZO (Proterozoic and later recycling of ocean crust during modern-style tectonics) mantle end members. Small portions of HIMU material could still be stored in

the SCLM and thus melting of Archean lithospheric mantle remaining in the lithosphere could also contribute to forming HIMU, i.e. it does not have to be derived from lower mantle plumes.

9. Acknowledgments

We thank the captains and crews of 1) the R/V SONNE for their support during cruises SO168-Zealandia, SO193-Manihiki and SO233-Walvis II, and 2) the R/V Maria S. Merian for their support during MSM19/3. S. Hauff, K. Junge, A. Schwindrofska, J. Sticklus, J. Rohde and U. Westernströer are gratefully acknowledged for analytical support; M. Anders for help with sample preparation; and C. Devey for providing sample SO84 86DS-1a from cruise SO84. We further thank J. D. Greenough and an anonymous reviewer for constructive comments that helped improve this manuscript. This study and SH's doctoral position were funded by the German Ministry for Research and Education (BMBF; grants SO233-Walvis II to KH and FH).

10. Funding

This work was funded by German Ministry for Research and Education (BMBF, grants SO168-Zealandia, SO193-Manihiki and SO233-Walvis II), German Research Association (DFG, grant MSM19/3); and the GEOMAR Helmholtz Center for Ocean Research Kiel.

11. Declaration of interest

Conflict of interest: none

References

Allègre, C. J., Moreira, M., and Staudacher, T., 1995, $^{4}He/^{3}He$ dispersion and mantle convection: Geophysical Research Letters, v. 22, no. 17, p. 2325-2328.

Baksi, A. K., 2007, A quantitative tool for detecting alteration in undisturbed rocks and minerals—I: Water, chemical weathering, and atmospheric argon: Geological Society of America Special Papers, v. 430, p. 285-303.

Bédard, J. H., 2006, A catalytic delamination-driven model for coupled genesis of Archaean crust and sub-continental lithospheric mantle: Geochimica et Cosmochimica Acta, v. 70, no. 5, p. 1188-1214.

-, 2018, Stagnant lids and mantle overturns: Implications for Archaean tectonics, magmagenesis, crustal growth, mantle evolution, and the start of plate tectonics: Geoscience Frontiers, v. 9, no. 1, p. 19-49.

Beiersdorf, H., Bach, W., Duncan, R., Erzinger, J., and Weiss, W., 1995, New evidence for the production of EM-type ocean island basalts and large volumes of volcaniclastites during the early history of the Manihiki Plateau: Marine Geology, v. 122, no. 3, p. 181-205.

Bell, K., 2001, Carbonatites: relationships to mantle-plume activity: SPECIAL PAPERS-GEOLOGICAL SOCIETY OF AMERICA, p. 267-290.

Bell, K., and Tilton, G. R., 2001, Nd, Pb and Sr Isotopic Compositions of East African Carbonatites: Evidence for Mantle Mixing and Plume Inhomogeneity: Journal of Petrology, v. 42, no. 10, p. 1927-1945.

Bradshaw, J. D., 1989, Cretaceous geotectonic patterns in the New Zealand Region: Tectonics, v. 8, no. 4, p. 803-820.

Burke, K., Steinberger, B., Torsvik, T. H., and Smethurst, M. A., 2008, Plume Generation Zones at the margins of Large Low Shear Velocity Provinces on the core–mantle boundary: Earth and Planetary Science Letters, v. 265, no. 1–2, p. 49-60.

Cabral, R. A., Jackson, M. G., Rose-Koga, E. F., Koga, K. T., Whitehouse, M. J., Antonelli, M. A., Farquhar, J., Day, J. M. D., and Hauri, E. H., 2013, Anomalous sulphur isotopes in plume lavas reveal deep mantle storage of Archaean crust: Nature, v. 496, no. 7446, p. 490-493.

Castillo, P. R., 2015, The recycling of marine carbonates and sources of HIMU and FOZO ocean island basalts: Lithos, v. 216-217, p. 254-263.

Castillo, P. R., Lonsdale, P. F., Moran, C. L., and Hawkins, J. W., 2009, Geochemistry of mid-Cretaceous Pacific crust being subducted along the Tonga–Kermadec Trench: Implications for the generation of arc lavas: Lithos, v. 112, no. 1–2, p. 87-102.

Chaffey, D. J., Cliff, R. A., and Wilson, B. M., 1989, Characterization of the St. Helena magma source: Magmatism in the Ocean Basins, v. 42, p. 19.

Chandler, M. T., Wessel, P., and Taylor, B., 2015, Tectonic reconstructions in magnetic quiet zones: Insights from the Greater Ontong Java Plateau: Geological Society of America Special Papers, v. 511, p. 185-193.

Chauvel, C., Hofmann, A. W., and Vidal, P., 1992, HIMU-EM : The French-Polynesian Connection: Earth and Planetary Science Letters, v. 110, no. 1-4, p. 99-119.

Chauvel, C., McDonough, W., Guille, G., Maury, R., and Duncan, R., 1997, Contrasting old and young volcanism in Rurutu Island, Austral chain: Chemical Geology, v. 139, no. 1–4, p. 125-143.

Class, C., and Goldstein, S. L., 2005, Evolution of helium isotopes in the Earth´s mantle: Nature, v. 436, p. 1107.

Collerson, K. D., Williams, Q., Ewart, A. E., and Murphy, D. T., 2010, Origin of HIMU and EM-1 domains sampled by ocean island basalts, kimberlites and carbonatites:

The role of CO2-fluxed lower mantle melting in thermochemical upwellings: Physics of the Earth and Planetary Interiors, v. 181, no. 3–4, p. 112-131.

Coltice, N., and Schmalzl, J., 2006, Mixing times in the mantle of the early Earth derived from 2-D and 3-D numerical simulations of convection: Geophysical Research Letters, v. 33, no. 23, p. n/a-n/a.

Condie, K. C., 2000, Episodic continental growth models: afterthoughts and extensions: Tectonophysics, v. 322, no. 1–2, p. 153-162.

Condie, K. C., and Kröner, A., 2008, When did plate tectonics begin? Evidence from the geologic record: Geological Society of America Special Papers, v. 440, p. 281-294.

Cooper, A. F., and Reid, D. L., 1998, Nepheline Sövites as Parental Magmas in Carbonatite Complexes: Evidence from Dicker Willem, Southwest Namibia: Journal of Petrology, v. 39, no. 11-12, p. 2123-2136.

Cooper, A. F., and Reid, D. L., 2000, The association of potassic trachytes and carbonatites at the Dicker Willem Complex, southwest Namibia: coexisting, immiscible, but not cogenetic magmas: Contributions to Mineralogy and Petrology, v. 139, no. 5, p. 570-583.

Dalton, J. A., and Presnall, D. C., 1998, The Continuum of Primary Carbonatitic–Kimberlitic Melt Compositions in Equilibrium with Lherzolite: Data from the System CaO–MgO–Al2O3–SiO2–CO2 at 6 GPa: Journal of Petrology, v. 39, no. 11-12, p. 1953-1964.

Dasgupta, R., Hirschmann, M. M., and Smith, N. D., 2007, Partial Melting Experiments of Peridotite + CO2 at 3 GPa and Genesis of Alkalic Ocean Island Basalts: Journal of Petrology, v. 48, no. 11, p. 2093-2124.

Dasgupta, R., Jackson, M. G., and Lee, C.-T. A., 2010, Major element chemistry of ocean island basalts — Conditions of mantle melting and heterogeneity of mantle source: Earth and Planetary Science Letters, v. 289, no. 3–4, p. 377-392.

Davy, B., Hoernle, K., and Werner, R., 2008, Hikurangi Plateau: Crustal structure, rifted formation, and Gondwana subduction history: Geochemistry, Geophysics, Geosystems, v. 9, no. 7, p. Q07004.

Dupuy, C., Barsczus, H. G., Dostal, J., Vidal, P., and Liotard, J. M., 1989, Subducted and recycled lithosphere as the mantle source of ocean island basalts from southern Polynesia, central Pacific: Chemical Geology, v. 77, no. 1, p. 1-18.

Finn, C. A., Müller, R. D., and Panter, K. S., 2005, A Cenozoic diffuse alkaline magmatic province (DAMP) in the southwest Pacific without rift or plume origin: Geochemistry, Geophysics, Geosystems, v. 6, no. 2, p. Q02005.

Foley, S. F., Buhre, S., and Jacob, D. E., 2003, Evolution of the Archaean crust by delamination and shallow subduction: Nature, v. 421, no. 6920, p. 249-252.

French, S. W., and Romanowicz, B., 2015, Broad plumes rooted at the base of the Earth's mantle beneath major hotspots: Nature, v. 525, no. 7567, p. 95-99.

Furman, T., Kaleta, K. M., Bryce, J. G., and Hanan, B. B., 2006, Tertiary Mafic Lavas of Turkana, Kenya: Constraints on East African Plume Structure and the Occurrence of High-μ Volcanism in Africa: Journal of Petrology, v. 47, no. 6, p. 1221-1244.

Gerbode, C., and Dasgupta, R., 2010, Carbonate-fluxed Melting of MORB-like Pyroxenite at 2·9 GPa and Genesis of HIMU Ocean Island Basalts: Journal of Petrology, v. 51, no. 10, p. 2067-2088.

Gerya, T., 2014, Precambrian geodynamics: Concepts and models: Gondwana Research, v. 25, no. 2, p. 442-463.

Gerya, T. V., Stern, R. J., Baes, M., Sobolev, S. V., and Whattam, S. A., 2015, Plate tectonics on the Earth triggered by plume-induced subduction initiation: Nature, v. 527, no. 7577, p. 221-225.

Golowin, R., Portnyagin, M., Hoernle, K., Hauff, F., Gurenko, A., Garbe-Schönberg, D., Werner, R., and Turner, S., 2017, Boninite-like intraplate magmas from Manihiki Plateau require ultra-depleted and enriched source components: Nature Communications, v. 8, p. 14322.

Graham, D. W., Humphris, S. E., Jenkins, W. J., and Kurz, M. D., 1992, Helium isotope geochemistry of some volcanic rocks from Saint Helena: Earth and Planetary Science Letters, v. 110, no. 1, p. 121-131.

Grégoire, M., Bell, D. R., and Le Roex, A. P., 2003, Garnet Lherzolites from the Kaapvaal Craton (South Africa): Trace Element Evidence for a Metasomatic History: Journal of Petrology, v. 44, no. 4, p. 629-657.

Gudfinnsson, G. H., and Presnall, D. C., 2005, Continuous gradations among primary carbonatitic, kimberlitic, melilititic, basaltic, picritic, and komatiitic melts in equilibrium with garnet lherzolite at 3–8 GPa: Journal of Petrology, v. 46, no. 8, p. 1645-1660.

Hanan, B. B., Blichert-Toft, J., Pyle, D. G., and Christie, D. M., 2004, Contrasting origins of the upper mantle revealed by hafnium and lead isotopes from the Southeast Indian Ridge: Nature, v. 432, no. 7013, p. 91-94.

Hanan, B. B., and Graham, D. W., 1996, Lead and Helium Isotope Evidence from Oceanic Basalts for a Common Deep Source of Mantle Plumes: Science, v. 272, no. 5264, p. 991-995.

Hanyu, T., Dosso, L., Ishizuka, O., Tani, K., Hanan, B. B., Adam, C., Nakai, S. i., Senda, R., Chang, Q., and Tatsumi, Y., 2013, Geochemical diversity in submarine HIMU basalts from Austral Islands, French Polynesia: Contributions to Mineralogy and Petrology, v. 166, no. 5, p. 1285-1304.

Hanyu, T., Kawabata, H., Tatsumi, Y., Kimura, J.-I., Hyodo, H., Sato, K., Miyazaki, T., Chang, Q., Hirahara, Y., Takahashi, T., Senda, R., and Nakai, S. i., 2014, Isotope evolution in the HIMU reservoir beneath St. Helena: Implications for the mantle recycling of U and Th: Geochimica et Cosmochimica Acta, v. 143, p. 232-252.

Hanyu, T., Tatsumi, Y., Senda, R., Miyazaki, T., Chang, Q., Hirahara, Y., Takahashi, T., Kawabata, H., Suzuki, K., Kimura, J. I., and Nakai, S., 2011, Geochemical characteristics and origin of the HIMU reservoir: A possible mantle plume source in the lower mantle: Geochemistry Geophysics Geosystems, v. 12.

Harris, L. B., and Bédard, J. H., 2014, Crustal Evolution and Deformation in a Non-Plate-Tectonic Archaean Earth: Comparisons with Venus, *in* Dilek, Y., and Furnes, H., eds., Evolution of Archean Crust and Early Life: Dordrecht, Springer Netherlands, p. 215-291.

Hart, S. R., 1984, A large-scale isotope anomaly in the Southern Hemisphere mantle: Nature, v. 309, no. 5971, p. 753-757.

Hart, S. R., Blusztajn, J., LeMasurier, W. E., and Rex, D. C., 1997, Hobbs Coast Cenozoic volcanism: Implications for the West Antarctic rift system: Chemical Geology, v. 139, no. 1-4, p. 223-248.

Hart, S. R., Gerlach, D. C., and White, W. M., 1986, A Possible New Sr-Nd-Pb Mantle Array and Consequences for Mantle Mixing: Geochimica Et Cosmochimica Acta, v. 50, no. 7, p. 1551-1557.

Hart, S. R., Hauri, E. H., Oschmann, L. A., and Whitehead, J. A., 1992, Mantle Plumes and Entrainment: Isotopic Evidence: Science, v. 256, no. 5056, p. 517-520.

Herzberg, C., 2014, Early Earth: Archaean drips: Nature Geosci, v. 7, no. 1, p. 7-8.

Herzberg, C., Cabral, R. A., Jackson, M. G., Vidito, C., Day, J. M. D., and Hauri, E. H., 2014, Phantom Archean crust in Mangaia hotspot lavas and the meaning of heterogeneous mantle: Earth and Planetary Science Letters, v. 396, p. 97-106.

Higgins, J. A., Fischer, W. W., and Schrag, D. P., 2009, Oxygenation of the ocean and sediments: Consequences for the seafloor carbonate factory: Earth and Planetary Science Letters, v. 284, no. 1–2, p. 25-33.

Hochmuth, K., Gohl, K., and Uenzelmann-Neben, G., 2015, Playing jigsaw with Large Igneous Provinces—A plate tectonic reconstruction of Ontong Java Nui, West Pacific: Geochemistry, Geophysics, Geosystems, v. 16, no. 11, p. 3789-3807.

Hoernle, K., Hauff, F., van den Bogaard, P., Werner, R., Mortimer, N., Geldmacher, J., Garbe-Schönberg, D., and Davy, B., 2010, Age and geochemistry of volcanic rocks from the Hikurangi and Manihiki oceanic Plateaus: Geochimica et Cosmochimica Acta, v. 74, no. 24, p. 7196-7219.

Hoernle, K., Mortimer, N., Werner, R., and Hauff, F., 2003, FS/RV SONNE Fahrtbericht SO 168= Cruise report SO168, ZEALANDIA: Causes and Effects of Plume and Rift-Related Cretaceous and Cenozoic Volcanism on Zealandia; Wellington-Sydney-Lyttleton/Christchurch; December 03, 2002-January 16, 2003;[BMBF contract No. 03G0168A].

Hoernle, K., Rohde, J., Hauff, F., Garbe-Schonberg, D., Homrighausen, S., Werner, R., and Morgan, J. P., 2015, How and when plume zonation appeared during the 132 Myr evolution of the Tristan Hotspot: Nature Communication, v. 6, p. 10.1038/ncomms8799.

Hoernle, K., Schwindrofska, A., Werner, R., van den Bogaard, P., Hauff, F., Uenzelmann-Neben, G., and Garbe-Schönberg, D., 2016, Tectonic dissection and displacement of parts of Shona hotspot volcano 3500 km along the Agulhas-Falkland Fracture Zone: Geology, v. 44, no. 4, p. 263-266.

Hoernle, K., Tilton, G., Le Bas, M. J., Duggen, S., and Garbe-Schönberg, D., 2002, Geochemistry of oceanic carbonatites compared with continental carbonatites: mantle recycling of oceanic crustal carbonate: Contributions to Mineralogy and Petrology, v. 142, no. 5, p. 520-542.

Hoernle, K., Tilton, G., and Schmincke, H.-U., 1991, Sr-Nd-Pb isotopic evolution of Gran Canaria: Evidence for shallow enriched mantle beneath the Canary Islands: Earth and Planetary Science Letters, v. 106, no. 1, p. 44-63.

Hoernle, K., Werner, R., and Lüter, C., 2014, RV SONNE Fahrtbericht/Cruise Report SO233 WALVIS II, 14.05-21.06. 2014, Cape Town, South Africa-Walvis Bay, Namibia: GEOMAR Report v. no. 23 (N. Ser.), p. 53 pp + Appendices.

Hoffman, N. R. A., and McKenzie, D. P., 1985, The destruction of geochemical heterogeneities by differential fluid motions during mantle convection: Geophysical Journal of the Royal Astronomical Society, v. 82, no. 2, p. 163-206.

Hofmann, A. W., 1988, Chemical Differentiation of the Earth - The Relationship between Mantle, Continental Crust, and Oceanic Crust: Earth and Planetary Science Letters, v. 90, no. 3, p. 297-314.

-, 1997, Mantle geochemistry: the message from oceanic volcanism: Nature, v. 385, no. 6613, p. 219-229.

Hofmann, A. W., Jochum, K. P., Seufert, M., and White, W. M., 1986, Nb and Pb in oceanic basalts: new constraints on mantle evolution: Earth and Planetary Science Letters, v. 79, no. 1, p. 33-45.

Hofmann, A. W., and White, W. M., 1982, Mantle plumes from ancient oceanic crust: Earth and Planetary Science Letters, v. 57, no. 2, p. 421-436.

Humphris, S. E., and Thompson, G., 1983, Geochemistry of rare earth elements in basalts from the Walvis Ridge: implications for its origin and evolution: Earth and Planetary Science Letters, v. 66, no. Supplement C, p. 223-242.

Ingle, S., Mahoney, J. J., Sato, H., Coffin, M. F., Kimura, J.-I., Hirano, N., and Nakanishi, M., 2007, Depleted mantle wedge and sediment fingerprint in unusual basalts from the Manihiki Plateau, central Pacific Ocean: Geology, v. 35, no. 7, p. 595-598.

Jackson, M., Cabral, R., Rose-Koga, E., Koga, K., Price, A., Hauri, E., and Michael, P., 2015, Ultra-depleted melts in olivine-hosted melt inclusions from the Ontong Java Plateau: Chemical Geology, v. 414, p. 124-137.

Jackson, M. G., Becker, T. W., and Konter, J. G., 2018, Evidence for a deep mantle source for EM and HIMU domains from integrated geochemical and geophysical constraints: Earth and Planetary Science Letters, v. 484, p. 154-167.

Jackson, M. G., and Dasgupta, R., 2008, Compositions of HIMU, EM1, and EM2 from global trends between radiogenic isotopes and major elements in ocean island basalts: Earth and Planetary Science Letters, v. 276, no. 1–2, p. 175-186.

Jackson, M. G., Hart, S. R., Konter, J. G., Koppers, A. A. P., Staudigel, H., Kurz, M. D., Blusztajn, J., and Sinton, J. M., 2010, Samoan hot spot track on a "hot spot highway": Implications for mantle plumes and a deep Samoan mantle source: Geochemistry, Geophysics, Geosystems, v. 11, no. 12, p. Q12009.

Jackson, M. G., Hart, S. R., Konter, J. G., Kurz, M. D., Blusztajn, J., and Farley, K. A., 2014, Helium and lead isotopes reveal the geochemical geometry of the Samoan plume: Nature, v. 514, no. 7522, p. 355-358.

Jackson, M. G., Hart, S. R., Saal, A. E., Shimizu, N., Kurz, M. D., Blusztajn, J. S., and Skovgaard, A. C., 2008, Globally elevated titanium, tantalum, and niobium (TITAN) in ocean island basalts with high 3He/4He: Geochemistry, Geophysics, Geosystems, v. 9, no. 4, p. n/a-n/a.

Jacob, D. E., and Foley, S. F., 1999, Evidence for Archean ocean crust with low high field strength element signature from diamondiferous eclogite xenoliths: Lithos, v. 48, no. 1–4, p. 317-336.

Janney, P. E., Le Roex, A. P., Carlson, R. W., and Viljoen, K. S., 2002, A Chemical and Multi-Isotope Study of the Western Cape Olivine Melilitite Province, South Africa: Implications for the Sources of Kimberlites and the Origin of the HIMU Signature in Africa: Journal of Petrology, v. 43, no. 12, p. 2339-2370.

Johnson, M. C., and Plank, T., 2000, Dehydration and melting experiments constrain the fate of subducted sediments: Geochemistry, Geophysics, Geosystems, v. 1, no. 12, p. n/a-n/a.

Johnson, T. E., Brown, M., Kaus, B. J. P., and VanTongeren, J. A., 2014, Delamination and recycling of Archaean crust caused by gravitational instabilities: Nature Geosci, v. 7, no. 1, p. 47-52.

Jourdan, F., Renne, P. R., and Reimold, W. U., 2009, An appraisal of the ages of terrestrial impact structures: Earth and Planetary Science Letters, v. 286, no. 1, p. 1-13.

Kalt, A., Hegner, E., and Satir, M., 1997, Nd, Sr, and Pb isotopic evidence for diverse lithospheric mantle sources of East African Rift carbonatites: Tectonophysics, v. 278, no. 1, p. 31-45.

Kaminsky, F., 2012, Mineralogy of the lower mantle: A review of 'super-deep' mineral inclusions in diamond: Earth-Science Reviews, v. 110, no. 1–4, p. 127-147.

Karsten, J. L., Klein, E. M., and Sherman, S. B., 1996, Subduction zone geochemical characteristics in ocean ridge basalts from the southern Chile Ridge: Implications of modern ridge subduction systems for the Archean: Lithos, v. 37, no. 2, p. 143-161.

Kawabata, H., Hanyu, T., Chang, Q., Kimura, J.-I., Nichols, A. R. L., and Tatsumi, Y., 2011, The Petrology and Geochemistry of St. Helena Alkali Basalts: Evaluation of the

Oceanic Crust-recycling Model for HIMU OIB: Journal of Petrology, v. 52, no. 4, p. 791-838.

Keller, J., Zaitsev, A. N., and Wiedenmann, D., 2006, Primary magmas at Oldoinyo Lengai: The role of olivine melilitites: Lithos, v. 91, no. 1–4, p. 150-172.

Kellogg, L. H., and Turcotte, D. L., 1990, Mixing and the distribution of heterogeneities in a chaotically convecting mantle: Journal of Geophysical Research: Solid Earth, v. 95, no. B1, p. 421-432.

Kimura, J.-I., Gill, J. B., Skora, S., van Keken, P. E., and Kawabata, H., 2016, Origin of geochemical mantle components: Role of subduction filter: Geochemistry, Geophysics, Geosystems, v. 17, no. 8, p. 3289-3325.

Kipf, A., Hauff, F., Werner, R., Gohl, K., van den Bogaard, P., Hoernle, K., Maicher, D., and Klügel, A., 2014, Seamounts off the West Antarctic margin: A case for non-hotspot driven intraplate volcanism: Gondwana Research, v. 25, no. 4, p. 1660-1679.

Kogiso, T., Hirose, K., and Takahashi, E., 1998, Melting experiments on homogeneous mixtures of peridotite and basalt: application to the genesis of ocean island basalts: Earth and Planetary Science Letters, v. 162, no. 1–4, p. 45-61.

Kogiso, T., and Hirschmann, M. M., 2006, Partial melting experiments of bimineralic eclogite and the role of recycled mafic oceanic crust in the genesis of ocean island basalts: Earth and Planetary Science Letters, v. 249, no. 3–4, p. 188-199.

Kogiso, T., Tatsumi, Y., and Nakano, S., 1997a, Trace element transport during dehydration processes in the subducted oceanic crust: 1. Experiments and implications for the origin of ocean island basalts: Earth and Planetary Science Letters, v. 148, no. 1, p. 193-205.

Kogiso, T., Tatsumi, Y., Shimoda, G., and Barsczus, H. G., 1997b, High μ (HIMU) ocean island basalts in southern Polynesia: New evidence for whole mantle scale recycling of subducted oceanic crust: Journal of Geophysical Research: Solid Earth, v. 102, no. B4, p. 8085-8103.

Konter, J. G., Hanan, B. B., Blichert-Toft, J., Koppers, A. A. P., Plank, T., and Staudigel, H., 2008, One hundred million years of mantle geochemical history suggest the retiring of mantle plumes is premature: Earth and Planetary Science Letters, v. 275, no. 3–4, p. 285-295.

Koppers, A. A. P., Staudigel, H., Christie, D. M., Dieu, J. J., and Pringle, M. S., 1995, Sr-Nd-Pb isotope geochemistry of Leg 144 West Pacific guyots; implications for the geochemical evolution of the "SOPITA" mantle anomaly: Proceedings of the Ocean Drilling Program, scientific results, Northwest Pacific atolls and guyots; covering Leg 144 of the cruises of the drilling vessel JOIDES Resolution, Majuro Atoll to Yokohama, Japan, sites 871-880 and Site 801, 19 May-20 July 1992, v. 144, p. 535.

Koppers, A. A. P., Staudigel, H., Pringle, M. S., and Wijbrans, J. R., 2003, Short-lived and discontinuous intraplate volcanism in the South Pacific: Hot spots or extensional volcanism?: Geochemistry, Geophysics, Geosystems, v. 4, no. 10, p. n/a-n/a.

Kramers, J. D., 1977, Lead and strontium isotopes in Cretaceous kimberlites and mantle-derived xenoliths from Southern Africa: Earth and Planetary Science Letters, v. 34, no. 3, p. 419-431.

Krystopowicz, N. J., and Currie, C. A., 2013, Crustal eclogitization and lithosphere delamination in orogens: Earth and Planetary Science Letters, v. 361, p. 195-207.

Kurz, M. D., Jenkins, W. J., and Hart, S. R., 1982, Helium isotopic systematics of oceanic islands and mantle heterogeneity: Nature, v. 297, no. 5861, p. 43-47.

Lanphere, M. A., and Dalrymple, G. B., 1978, The use of 40Ar/39Ar data in evaluation of disturbed K-Ar systems: Geological Survey Open-File Report 78-701, p. 141-148.

Lassiter, J. C., Blichert-Toft, J., Hauri, E. H., and Barsczus, H. G., 2003, Isotope and trace element variations in lavas from Raivavae and Rapa, Cook–Austral islands: constraints on the nature of HIMU- and EM-mantle and the origin of mid-plate volcanism in French Polynesia: Chemical Geology, v. 202, no. 1–2, p. 115-138.

Le Maitre, R. W., Streckeisen, A., Zanettin, B., Le Bas, M., Bonin, B., and Bateman, P., 2005, Igneous rocks: a classification and glossary of terms: recommendations of the International Union of Geological Sciences Subcommission on the Systematics of Igneous Rocks, Cambridge University Press.

Le Roex, A., Class, C., O'Connor, J., and Jokat, W., 2010, Shona and Discovery Aseismic Ridge Systems, South Atlantic: Trace Element Evidence for Enriched Mantle Sources: Journal of Petrology, v. 51, no. 10, p. 2089-2120.

Lee, C. T. A., 2006, Geochemical/petrologic constraints on the origin of cratonic mantle: Archean geodynamics and environments, p. 89-114.

Lucassen, F., Franz, G., Romer, R. L., Pudlo, D., and Dulski, P., 2008, Nd, Pb, and Sr isotope composition of Late Mesozoic to Quaternary intra-plate magmatism in NE-Africa (Sudan, Egypt): high-μ signatures from the mantle lithosphere: Contributions to Mineralogy and Petrology, v. 156, no. 6, p. 765-784.

MacDonald, G. A., 1968, Composition and Origin of Hawaiian Lavas: Geological Society of America Memoirs, v. 116, p. 477-522.

Mallik, A., and Dasgupta, R., 2012, Reaction between MORB-eclogite derived melts and fertile peridotite and generation of ocean island basalts: Earth and Planetary Science Letters, v. 329–330, p. 97-108.

-, 2013, Reactive Infiltration of MORB-Eclogite-Derived Carbonated Silicate Melt into Fertile Peridotite at 3 GPa and Genesis of Alkalic Magmas: Journal of Petrology, v. 54, no. 11, p. 2267-2300.

-, 2014, Effect of variable CO2 on eclogite-derived andesite and lherzolite reaction at 3 GPa—Implications for mantle source characteristics of alkalic ocean island basalts: Geochemistry, Geophysics, Geosystems, v. 15, no. 4, p. 1533-1557.

Mana, S., Furman, T., Carr, M. J., Mollel, G. F., Mortlock, R. A., Feigenson, M. D., Turrin, B. D., and Swisher Iii, C. C., 2012, Geochronology and geochemistry of the Essimingor volcano: Melting of metasomatized lithospheric mantle beneath the North Tanzanian Divergence zone (East African Rift): Lithos, v. 155, p. 310-325.

Manikyamba, C., and Kerrich, R., 2011, Geochemistry of alkaline basalts and associated high-Mg basalts from the 2.7Ga Penakacherla Terrane, Dharwar craton, India: An Archean depleted mantle-OIB array: Precambrian Research, v. 188, no. 1, p. 104-122.

Maury, R. C., Guille, G., Guillou, H., Chauvel, C., Rossi, P., Pallares, C., and Legendre, C., 2013, Temporal evolution of a Polynesian hotspot: New evidence from Raivavae (Austral islands, South Pacific ocean): Bulletin de la Societe Geologique de France, v. 184, p. 557-567.

McCoy-West, A. J., Bennett, V. C., and Amelin, Y., 2016, Rapid Cenozoic ingrowth of isotopic signatures simulating "HIMU" in ancient lithospheric mantle: Distinguishing source from process: Geochimica et Cosmochimica Acta, v. 187, p. 79-101.

McCulloch, M. T., and Bennett, V. C., 1994, Progressive growth of the Earth's continental crust and depleted mantle: Geochemical constraints: Geochimica et Cosmochimica Acta, v. 58, no. 21, p. 4717-4738.

McDonough, W. F., 1990, Constraints on the composition of the continental lithospheric mantle: Earth and Planetary Science Letters, v. 101, no. 1, p. 1-18.

Montelli, R., Nolet, G., Dahlen, F. A., and Masters, G., 2006, A catalogue of deep mantle plumes: New results from finite-frequency tomography: Geochemistry, Geophysics, Geosystems, v. 7, no. 11, p. Q11007.

Moore, K. R., and Wood, B. J., 1998, The Transition from Carbonate to Silicate Melts in the CaO—MgO—SiO2—CO2 System: Journal of Petrology, v. 39, no. 11-12, p. 1943-1951.

Morgan, W. J., 1971, Convection Plumes in the Lower Mantle: Nature, v. 230, no. 5288, p. 42-43.

Moyen, J.-F., and Laurent, O., 2018, Archaean tectonic systems: A view from igneous rocks: Lithos, v. 302-303, p. 99-125.

Nebel, O., Arculus, R. J., van Westrenen, W., Woodhead, J. D., Jenner, F. E., Nebel-Jacobsen, Y. J., Wille, M., and Eggins, S. M., 2013, Coupled Hf–Nd–Pb isotope co-variations of HIMU oceanic island basalts from Mangaia, Cook-Austral islands, suggest an Archean source component in the mantle transition zone: Geochimica et Cosmochimica Acta, v. 112, p. 87-101.

Nelson, D. R., Chivas, A. R., Chappell, B. W., and McCulloch, M. T., 1988, Geochemical and isotopic systematics in carbonatites and implications for the evolution of ocean-island sources: Geochimica et Cosmochimica Acta, v. 52, no. 1, p. 1-17.

Nowell, G. M., Pearson, D. G., Bell, D. R., Carlson, R. W., Smith, C. B., Kempton, P. D., and Noble, S. R., 2004, Hf Isotope Systematics of Kimberlites and their Megacrysts: New Constraints on their Source Regions: Journal of Petrology, v. 45, no. 8, p. 1583-1612.

O'Connor, J. M., and Duncan, R. A., 1990, Evolution of the Walvis Ridge-Rio Grande Rise Hot Spot System: Implications for African and South American Plate motions over plumes: Journal of Geophysical Research: Solid Earth, v. 95, no. B11, p. 17475-17502.

O'Connor, J. M., and Jokat, W., 2015a, Tracking the Tristan-Gough mantle plume using discrete chains of intraplate volcanic centers buried in the Walvis Ridge: Geology, v. 43, no. 8, p. 715-718.

-, 2015b, Age distribution of Ocean Drill sites across the Central Walvis Ridge indicates plate boundary control of plume volcanism in the South Atlantic: Earth and Planetary Science Letters, v. 424, p. 179-190.

O'Connor, J. M., Jokat, W., le Roex, A. P., Class, C., Wijbrans, J. R., Keszling, S., Kuiper, K. F., and Nebel, O., 2012, Hotspot trails in the South Atlantic controlled by plume and plate tectonic processes: Nature Geoscience, v. 5, no. 10, p. 735-738.

O'Neill, C., Lenardic, A., Moresi, L., Torsvik, T. H., and Lee, C. T. A., 2007, Episodic Precambrian subduction: Earth and Planetary Science Letters, v. 262, no. 3–4, p. 552-562.

Panter, K. S., Blusztajn, J., Hart, S. R., Kyle, P. R., Esser, R., and McIntosh, W. C., 2006, The origin of HIMU in the SW Pacific: Evidence from intraplate volcanism in southern New Zealand and subantarctic islands: Journal of Petrology, v. 47, no. 9, p. 1673-1704.

Panter, K. S., Hart, S. R., Kyle, P., Blusztanjn, J., and Wilch, T., 2000, Geochemistry of Late Cenozoic basalts from the Crary Mountains: characterization of mantle sources in Marie Byrd Land, Antarctica: Chemical Geology, v. 165, no. 3–4, p. 215-241.

Paslick, C., Halliday, A., James, D., and Dawson, J. B., 1995, Enrichment of the continental lithosphere by OIB melts: Isotopic evidence from the volcanic province of northern Tanzania: Earth and Planetary Science Letters, v. 130, no. 1, p. 109-126.

Pearce, J. A., 1996, A user's guide to basalt discrimination diagrams: Trace element geochemistry of volcanic rocks: applications for massive sulphide exploration. Geological Association of Canada, Short Course Notes, v. 12, no. 79, p. 113.

Pertermann, M., and Hirschmann, M. M., 2003, Partial melting experiments on a MORB-like pyroxenite between 2 and 3 GPa: Constraints on the presence of pyroxenite in basalt source regions from solidus location and melting rate: Journal of Geophysical Research: Solid Earth, v. 108, no. B2.

Pietsch, R., and Uenzelmann-Neben, G., 2015, The Manihiki Plateau—A multistage volcanic emplacement history: Geochemistry, Geophysics, Geosystems, v. 16, no. 8, p. 2480-2498.

Pilet, S., Hernandez, J., Sylvester, P., and Poujol, M., 2005, The metasomatic alternative for ocean island basalt chemical heterogeneity: Earth and Planetary Science Letters, v. 236, no. 1, p. 148-166.

Plank, T., and Langmuir, C. H., 1998, The chemical composition of subducting sediment and its consequences for the crust and mantle: Chemical Geology, v. 145, no. 3–4, p. 325-394.

Pringle, M. S., Sager, W. W., Sliter, W. V., and Stein, S., 1993, The Mesozoic Pacific: Geology, Tectonics, and Volcanism: A Volume in Memory of Sy Schlanger: Washington DC American Geophysical Union Geophysical Monograph Series, v. 77.

Ren, Z.-Y., Hanyu, T., Miyazaki, T., Chang, Q., Kawabata, H., Takahashi, T., Hirahara, Y., Nichols, A. R. L., and Tatsumi, Y., 2009, Geochemical Differences of the Hawaiian Shield Lavas: Implications for Melting Process in the Heterogeneous Hawaiian Plume: Journal of Petrology, v. 50, no. 8, p. 1553-1573.

Renne, P. R., Glen, J. M., Milner, S. C., and Duncan, A. R., 1996, Age of Etendeka flood volcanism and associated intrusions in southwestern Africa: Geology, v. 24, no. 7, p. 659-662.

Richards, M. A., Duncan, R. A., and Courtillot, V. E., 1989, Flood basalts and hot-spot tracks: plume heads and tails: Science, v. 246, no. 4926, p. 103-107.

Richardson, S. H., Erlank, A. J., Duncan, A. R., and Reid, D. L., 1982, Correlated Nd, Sr and Pb Isotope Variation in Walvis Ridge Basalts and Implications for the Evolution of their Mantle Source: Earth and Planetary Science Letters, v. 59, no. 2, p. 327-342.

Richardson, S. H., Erlank, A. J., Reid, D. L., and Duncan, A. R., 1984, Major and Trace-Elements and Nd and Sr Isotope Geochemistry of Basalts from the Deep-Sea Drilling Project Leg-74 Walvis Ridge Transect: Initial Reports of the Deep Sea Drilling Project, v. 74, no. Mar, p. 739-754.

Rino, S., Komiya, T., Windley, B. F., Katayama, I., Motoki, A., and Hirata, T., 2004, Major episodic increases of continental crustal growth determined from zircon ages of river sands; implications for mantle overturns in the Early Precambrian: Physics of the Earth and Planetary Interiors, v. 146, no. 1–2, p. 369-394.

Roex, A. P., Späth, A., and Zartman, R. E., 2001, Lithospheric thickness beneath the southern Kenya Rift: implications from basalt geochemistry: Contributions to Mineralogy and Petrology, v. 142, no. 1, p. 89-106.

Rogers, N., Macdonald, R., Fitton, J. G., George, R., Smith, M., and Barreiro, B., 2000, Two mantle plumes beneath the East African rift system: Sr, Nd and Pb isotope evidence from Kenya Rift basalts: Earth and Planetary Science Letters, v. 176, no. 3–4, p. 387-400.

Rohde, J., Hoernle, K., Hauff, F., Werner, R., O'Connor, J., Class, C., Garbe-Schönberg, D., and Jokat, W., 2013a, 70 Ma chemical zonation of the Tristan-Gough hotspot track: Geology, v. 43, no. 3, p. 335-338.

Rohde, J. K., van den Bogaard, P., Hoernle, K., Hauff, F., and Werner, R., 2013b, Evidence for an age progression along the Tristan-Gough volcanic track from new 40Ar/39Ar ages on phenocryst phases: Tectonophysics, v. 604, p. 60-71.

Rooney, T. O., Nelson, W. R., Dosso, L., Furman, T., and Hanan, B., 2014, The role of continental lithosphere metasomes in the production of HIMU-like magmatism on the northeast African and Arabian plates: Geology, v. 42(5), p. 419-422.

Saal, A. E., Hart, S. R., Shimizu, N., Hauri, E. H., and Layne, G. D., 1998, Pb Isotopic Variability in Melt Inclusions from Oceanic Island Basalts, Polynesia: Science, v. 282, p. 1481-1484.

Said, N., and Kerrich, R., 2010, Magnesian dyke suites of the 2.7Ga Kambalda Sequence, Western Australia: Evidence for coeval melting of plume asthenosphere and metasomatised lithospheric mantle: Precambrian Research, v. 180, no. 3, p. 183-203.

Salters, V. J. M., Mallick, S., Hart, S. R., Langmuir, C. E., and Stracke, A., 2011, Domains of depleted mantle: New evidence from hafnium and neodymium isotopes: Geochemistry, Geophysics, Geosystems, v. 12, no. 8, p. n/a-n/a.

Salters, V. J. M., and Sachi-Kocher, A., 2010, An ancient metasomatic source for the Walvis Ridge basalts: Chemical Geology, v. 273, no. 3–4, p. 151-167.

Salters, V. J. M., and Stracke, A., 2004, Composition of the depleted mantle: Geochemistry, Geophysics, Geosystems, v. 5, no. 5, p. Q05B07.

Schiano, P., Burton, K. W., Dupré, B., Birck, J. L., Guille, G., and Allègre, C. J., 2001, Correlated Os–Pb–Nd–Sr isotopes in the Austral–Cook chain basalts: the nature of mantle components in plume sources: Earth and Planetary Science Letters, v. 186, no. 3–4, p. 527-537.

Schlömer, A., Geissler, W. H., Jokat, W., and Jegen, M., 2017, Hunting for the Tristan mantle plume – An upper mantle tomography around the volcanic island of Tristan da Cunha: Earth and Planetary Science Letters, v. 462, p. 122-131.

Shirey, S. B., and Richardson, S. H., 2011, Start of the Wilson Cycle at 3 Ga Shown by Diamonds from Subcontinental Mantle: Science, v. 333, no. 6041, p. 434-436.

Simonetti, A., and Bell, K., 1995, Nd, Pb and Sr Isotopic Data from the Mount-Elgon Volcano, Eastern Uganda Western Kenya - Implications for the Origin and Evolution of Nephelinite Lavas: Lithos, v. 36, no. 2, p. 141-153.

Smith, W. H. F., Staudigel, H., Watts, A. B., and Pringle, M. S., 1989, The Magellan seamounts: Early Cretaceous record of the South Pacific isotopic and thermal anomaly: Journal of Geophysical Research: Solid Earth, v. 94, no. B8, p. 10501-10523.

Spandler, C., Yaxley, G., Green, D. H., and Rosenthal, A., 2008, Phase Relations and Melting of Anhydrous K-bearing Eclogite from 1200 to 1600°C and 3 to 5 GPa: Journal of Petrology, v. 49, no. 4, p. 771-795.

Staudigel, H., Park, K. H., Pringle, M., Rubenstone, J. L., Smith, W. H. F., and Zindler, A., 1991, The longevity of the South Pacific isotopic and thermal anomaly: Earth and Planetary Science Letters, v. 102, no. 1, p. 24-44.

Steiger, R. H., and Jäger, E., 1977, Subcommission on geochronology: Convention on the use of decay constants in geo- and cosmochronology: Earth and Planetary Science Letters, v. 36, no. 3, p. 359-362.

Stein, M., and Hofmann, A. W., 1994, Mantle plumes and episodic crustal growth: Nature, v. 372, no. 6501, p. 63-68.

Stein, M., Navon, O., and Kessel, R., 1997, Chromatographic metasomatism of the Arabian—Nubian lithosphere: Earth and Planetary Science Letters, v. 152, no. 1–4, p. 75-91.

Steinberger, B., and Torsvik, T. H., 2012, A geodynamic model of plumes from the margins of Large Low Shear Velocity Provinces: Geochemistry, Geophysics, Geosystems, v. 13, no. 1, p. Q01W09.

Stewart, K., and Rogers, N., 1996, Mantle plume and lithosphere contributions to basalts from southern Ethiopia: Earth and Planetary Science Letters, v. 139, no. 1-2, p. 195-211.

Storey, B. C., Leat, P. T., Weaver, S. D., Pankhurst, R. J., Bradshaw, J. D., and Kelley, S., 1999, Mantle plumes and Antarctica-New Zealand rifting: evidence from mid-Cretaceous mafic dykes: Journal of the Geological Society, v. 156, no. 4, p. 659-671.

Stracke, A., 2012, Earth's heterogeneous mantle: A product of convection-driven interaction between crust and mantle: Chemical Geology, v. 330–331, p. 274-299.

Stracke, A., Bizimis, M., and Salters, V. J. M., 2003, Recycling oceanic crust: Quantitative constraints: Geochemistry, Geophysics, Geosystems, v. 4, no. 3, p. 8003.

Stracke, A., Hofmann, A. W., and Hart, S. R., 2005, FOZO, HIMU, and the rest of the mantle zoo: Geochemistry, Geophysics, Geosystems, v. 6, no. 5, p. Q05007.

Stroncik, N. A., Trumbull, R. B., Krienitz, M.-S., Niedermann, S., Romer, R. L., Harris, C., and Day, J., 2017, Helium isotope evidence for a deep-seated mantle plume involved in South Atlantic breakup: Geology, v. 45, no. 9, p. 827-830.

Sumino, H., Kaneoka, I., Matsufuji, K., and Sobolev, A. V., 2006, Deep mantle origin of kimberlite magmas revealed by neon isotopes: Geophysical Research Letters, v. 33, no. 16, p. n/a-n/a.

Sumner, D. Y., and Grotzinger, J. P., 1996, Were kinetics of Archean calcium carbonate precipitation related to oxygen concentration?: Geology, v. 24, no. 2, p. 119-122.

Tatsumoto, M., 1978, Isotopic composition of lead in oceanic basalt and its implication to mantle evolution: Earth and Planetary Science Letters, v. 38, no. 1, p. 63-87.

Taylor, B., 2006, The single largest oceanic plateau: Ontong Java–Manihiki–Hikurangi: Earth and Planetary Science Letters, v. 241, no. 3–4, p. 372-380.

Tejada, M. L. G., Mahoney, J. J., Duncan, R. A., and Hawkins, M. P., 1996, Age and Geochemistry of Basement and Alkalic Rocks of Malaita and Santa Isabel, Solomon Islands, Southern Margin of Ontong Java Plateau: Journal of Petrology, v. 37, no. 2, p. 361-394.

Tejada, M. L. G., Mahoney, J. J., Neal, C. R., Duncan, R. A., and Petterson, M. G., 2002, Basement Geochemistry and Geochronology of Central Malaita, Solomon Islands, with Implications for the Origin and Evolution of the Ontong Java Plateau: Journal of Petrology, v. 43, no. 3, p. 449-484.

Thirlwall, M. F., 1997, Pb isotopic and elemental evidence for OIB derivation from young HIMU mantle: Chemical Geology, v. 139, no. 1, p. 51-74.

Thompson, G., and Humphris, S., 1984, Petrology and Geochemistry of rocks from the Walvis Ridge-Deep-Sea Drilling Project Leg-74, Site525, Site527 and Site528 Initial Reports of the Deep Sea Drilling Project, v. 74, no. MAR, p. 755-764.

Timm, C., Hoernle, K., Werner, R., Hauff, F., den Bogaard, P. v., Michael, P., Coffin, M. F., and Koppers, A., 2011, Age and geochemistry of the oceanic Manihiki Plateau, SW Pacific: New evidence for a plume origin: Earth and Planetary Science Letters, v. 304, no. 1–2, p. 135-146.

Timm, C., Hoernle, K., Werner, R., Hauff, F., den Bogaard, P. v., White, J., Mortimer, N., and Garbe-Schönberg, D., 2010, Temporal and geochemical evolution of the Cenozoic intraplate volcanism of Zealandia: Earth-Science Reviews, v. 98, no. 1–2, p. 38-64.

Torsvik, T. H., Burke, K., Steinberger, B., Webb, S. J., and Ashwal, L. D., 2010, Diamonds sampled by plumes from the core-mantle boundary: Nature, v. 466, no. 7304, p. 352-355.

Torsvik, T. H., Smethurst, M. A., Burke, K., and Steinberger, B., 2006, Large igneous provinces generated from the margins of the large low-velocity provinces in the deep mantle: Geophysical Journal International, v. 167, no. 3, p. 1447-1460.

van den Bogaard, P., 2013, The origin of the Canary Island Seamount Province - New ages of old seamounts: Scientific Reports, v. 3, p. 2107.

van Keken, P. E., Hauri, E. H., and Ballentine, C. J., 2002, Mantle Mixing: The Generation, Preservation, and Destruction of Chemical Heterogeneity: Annual Review of Earth and Planetary Sciences, v. 30, no. 1, p. 493-525.

Van Kranendonk, M. J., 2010, Two types of Archean continental crust: Plume and plate tectonics on early Earth: American Journal of Science, v. 310, no. 10, p. 1187-1209.

Vollmer, R., and Norry, M. J., 1983, Unusual isotopic variations in Nyiragongo nephelinites: Nature, v. 301, no. 5896, p. 141-143.

Weaver, S. D., Storey, B. C., Pankhurst, R. J., Mukasa, S. B., DiVenere, V. J., and Bradshaw, J. D., 1994, Antarctica-New Zealand rifting and Marie Byrd Land lithospheric magmatism linked to ridge subduction and mantle plume activity: Geology, v. 22, no. 9, p. 811-814.

Weiss, Y., Class, C., Goldstein, S. L., and Hanyu, T., 2016, Key new pieces of the HIMU puzzle from olivines and diamond inclusions: Nature, v. 537, p. 666-670.

Weiss, Y., Griffin, W. L., Bell, D. R., and Navon, O., 2011, High-Mg carbonatitic melts in diamonds, kimberlites and the sub-continental lithosphere: Earth and Planetary Science Letters, v. 309, no. 3–4, p. 337-347.

Werner, R., and Hauff, F., 2007, FS Sonne/Fahrtbericht/Cruise Report SO 193: MANIHIKI Temporal, Spatial, and Tectonic Evolution of Oceanic Plateaus: IFMGEOMAR Report, v. 13.

White, W. M., 2015, Isotopes, DUPAL, LLSVPs, and Anekantavada: Chemical Geology, v. 419, p. 10-28.

Willbold, M., and Stracke, A., 2006, Trace element composition of mantle end-members: Implications for recycling of oceanic and upper and lower continental crust: Geochemistry, Geophysics, Geosystems, v. 7, no. 4, p. Q04004.

Wilson, J. T., 1963, Evidence from Islands on the Spreading of Ocean Floors: Nature, v. 197, no. 4867, p. 536-538.

Woodhead, J. D., 1996, Extreme HIMU in an oceanic setting: the geochemistry of Mangaia Island (Polynesia), and temporal evolution of the Cook—Austral hotspot: Journal of Volcanology and Geothermal Research, v. 72, no. 1, p. 1-19.

Workman, R. K., and Hart, S. R., 2005, Major and trace element composition of the depleted MORB mantle (DMM): Earth and Planetary Science Letters, v. 231, no. 1–2, p. 53-72.

Zindler, A., and Hart, S. R., 1986, Chemical Geodynamics: Annual Review of Earth and Planetary Sciences, v. 14, no. 1, p. 493-571.